Vibrotactile Sensory Feedback for Lower Limb Prostheses

Iris S. Jiang

A dissertation

submitted in partial fulfillment of the

requirements for the degree of

Doctor of Philosophy

University of Washington

2015

Reading Committee:

Blake Hannaford, Chair

Colin Studholme

Pierre Mourad

Program Authorized to Offer Degree:

Bioengineering

University of Washington

Abstract

Vibrotactile Sensory Feedback for Lower Limb Prostheses

Iris S. Jiang

Chair of the Supervisory Committee:
Professor Blake Hannaford
Electrical Engineering

This dissertation focuses on understanding the limitations of a vibrotactile feedback system on the thigh. Due to the dynamic nature of the environment and time-sensitive information that need to be relayed to the user, it is important to know the strengths and weaknesses of implementing a vibrotactile system. Our data showed that vibrotactile stimuli does not provide the fastest reaction time when compared to visual and auditory stimuli. In addition, vibrotactile stimuli of the lower limb was most affected when walking was introduced.

While investigating this issue, a systematic approach to understand human capability of spatially localizing perception was also developed. We found an interesting result that people were better at discriminating sensations mediolaterally than in the proximal/distal direction.

Based on our results, the use of a sensory substitution system may not be feasible unless movements are predicted or time-sensitive information is not being communicated. However, the sensory effects of targeted muscle reinnervation could be leveraged to make a vibrotactile feedback system that provides natural feedback instead of using sensory substitution methods of feedback.

TABLE OF CONTENTS

LIST OF FIGURES

LIST OF TABLES

ACKNOWLEDGEMENTS

I would like to express my sincerest gratitude to Blake for being a great advisor by helping me navigate through the twists and turns of research and complete this degree. You have supported my ideas, challenged my reasoning, and made me a better researcher and engineer.

Howard, you were like a second advisor to me (one that I never had to worry about during exams) and I greatly appreciate all of your advice over the years.

Thank you to my Reading Committee Blake Hannaford, Pierre Mourad, Colin Studholme as well as the rest of my Supervisory Committee Chet Moritz and Joan Sanders who took the time to come to my exams and provide valuable feedback.

Thank you to all the members of the BioRobotics Laboratory – Fredrik, Lee, Jeff, Andy, Kevin, Hawkeye, Tamara, Sharon, Paul, et al. – that have taken me under their wing, taught me everything I know about robots, provided great feedback, participated in data collection, and made the day-to-day life just that much more enjoyable.

I would like to thank the CSNE not only for funding my research but also for providing the invaluable experiences that have made my graduate career unique and memorable.

I would like to thank the friends I've made throughout the years in grad school. You have all helped make this journey incredibly amazing and I have learned so much more because of you.

Most importantly, I'd like to thank Rich, my Domokun, for always being there, even when the travelling got tough. You inspire me to do the things I never thought I wanted do, and guide me with your love and support.

DEDICATION

To my family

Chapter 1. INTRODUCTION

The ability to walk upright on two legs requires an intricate sensorimotor system to maintain balance, ambulate, and adapt to the physical environment [1]. The Central Nervous System (CNS) uses sensory feedback in two fundamentally different ways. Motor commands are integrated with afferent feedback during muscle activity, and the CNS expects to receive sensory information to ensure proper movement control. This also means less central input is necessary to activate the motoneurons when there is afferent sensory feedback. The other form of sensory feedback is generated when an unpredicted disturbance of the movement (or change in expected sensory feedback) occurs. This triggers a reflex burst to help correct the movement and avoid falling. Study of pathologies such as sensory neuropathy syndrome, which causes patients to suffer from partial or acute loss of proprioception and touch sensation, shows that some people are able to re-learn to walk despite the missing feedback. However, gait kinematics are drastically different, there is an increased dependence on visual feedback, and a greater demand on cognitive attention [2].

Amputation is another instance where the patient loses peripheral sensory mechanisms such as mechanoreceptors at the skin and proprioceptors in the muscles and joints. Globally, there are about 1 million amputations per year and currently 1.7 million amputees in the US alone [3], [4]. People with lower limb amputations often have reduced ability to navigate their surroundings and respond to sudden perturbations [5]. Part of the problem is a lack of control over prosthetic limbs, but an often overlooked aspect is the lack of sensory feedback when using a prosthetic leg [6].

When amputees go through rehabilitation training and learn how to walk with a prosthetic leg, there is complex cortical reorganization of postural and movement control that adjusts to the new mechanics [7]–[9]. They must learn the dynamic response properties of the prosthetic limb and how to indirectly control the leg based on new types of feedback.

Current advanced prosthetic legs on the market are generally focused on automated actuation such as mechatronic systems in ankles and/or knees, but none have a sensory feedback component [10], [11]. To compensate for the lack of sensory feedback, prosthesis wearers must rely on other sensory information such as forces that can be felt through the socket or visual cues of whether the ground is uneven or slippery. Amputees from the Harborview Medical Center amputee support group (Tuesdays at 11am) reported that they became more confident with walking over time.

However, they are still worried about tripping when navigating through crowds of people and on unanticipated slippery surfaces. The combination of multiple possible perturbations with the absence of line of sight of the prosthetic leg creates a particularly hazardous situation for amputees.

52% of amputees using prostheses have reported falling in the previous 12 months of use [12]. Poor ability to use a prosthetic leg often leads to a fear of falling and decreased balance confidence, which decreases an amputee's motivation to walk and is debilitating to both physical and psychological recovery. By choosing to not walk, amputees who fear falling often taken longer to regain independence. Additionally, they also tend to withdraw from social participation due to their lack of confidence in their walking ability [13]–[15].

Decreased ability to walk is one concern of amputees, while another equally important phenomenon that can affect quality of life is phantom limb pain. 98% of amputees develop a phantom limb effect after amputation, and sometimes this effect can be severe pain on the missing limb [7], [16]–[18]. The severity and frequency of the pain varies from patient to patient, but can be debilitating and cause tremendous distress upon the amputee on a daily basis. The cause of phantom limb sensation is not well understood, but it is often attributed to the misrepresentation of one's mental representation of his or her body after an amputation [7], [16], [19], [20]. Though there is no physiological proof of why phantom limb pain exists, multiple studies have shown that providing somatosensory feedback of the missing limb can ameliorate this pain [21]–[24]. This benefit alone highlights the importance of why prostheses with integrated tactile feedback would be such a crucial development for the field.

Sensory feedback systems typically fall into two categories: 1) Sensory Substitution - transforming characteristics of one sensory modality into stimuli for a different sensory modality (e.g. Braille for the blind). 2) Sensory Augmentation - providing feedback for a sense that humans do not normally possess (e.g. being able to feel magnetic fields in the environment through vibration). In either case, feedback is usually presented by either visual, auditory, or tactile stimulation. Non-invasive tactile stimulation methods include motor driven actuators, vibrotactile actuators, surface electrodes, piezoelectric actuators, shape memory alloys, rheological fluids, hydraulic actuators, and pneumatically driven actuators. Many of these methods are not practical to use as a wearable feedback system due to their limitations such as adaptation effects, slow response time, low force output, and having bulky/heavy mechanical apparatus. Consequently,

most research on sensory feedback for prostheses have focused on vibrotactile actuators and only a few have forayed into using electrotactile and pneumatic actuators.

A variety of researchers have seen that the use of vibrotactile feedback of sway on the torso successfully improved balance and posture [25]–[30]. Asseman found limited effectiveness of vibrotactile feedback on the head to trigger a compensatory step response [31], [32]. Studies that specifically focus on feedback to the lower limb have used electrotactile [33], [34], pneumatic [35], [36], and vibrotactile actuators [5], [37]–[39]. Fan's pneumatic actuators achieved 99% accuracy but were mechanically too slow, and took subjects almost 1-2 seconds to respond [35], [36]. Wentink's use of electrotactile feedback of a trip occurrence did not improve reaction time compared to no feedback [33]. Rusaw also did not see significant improvement of balance when amputees received vibrotactile feedback on the thigh [5]. Though none of these researchers have yet found sensory feedback to be significantly useful, it is possible that the right applications or feedback display has not been found.

Crea's study is the only thigh vibration experiment performed while walking. This experiment provided gait phase information to the thigh and found that people could perceive when the feedback became asynchronous [37]. While Sharma and Wentink provided a comprehensive study of the sensorimotor responses of vibration on the thigh, both studies were not performed while walking [33], [39]. Walking will introduce an extra cognitive load and the natural vibrations caused while walking could interfere with the vibrotactile motors. It is well known that changing from static to dynamic conditions also changes the perception thresholds of mechanical stimulations on the skin [40]. Since feedback mechanisms for prosthetic legs would be used during ambulation, it is important to ascertain how walking affects perception of vibration motors.

This dissertation focuses on understanding the limitations of a vibrotactile feedback system on the thigh. Due to the dynamic nature of the environment and time-sensitive information that needs to be relayed to the user, it is important to know the strengths and weaknesses of implementing a vibrotactile system. While investigating this issue, I also developed a systematic approach to understand human capability of spatially localizing perception in the hopes that this information can be used to create natural sensory feedback displays. The main contributions of this dissertation include:

-Development of a model to optimize vibrotactile support structures on the skin.

-Evaluation of human response capabilities to vibrotactile stimulation while walking.

-Development of a systematic approach to study sensory localization.

This dissertation is organized into six chapters. This first chapter provides an overview of the field and highlights the information missing from literature. Chapter 2 looks at vibrotactile actuators and how we improved the interface to optimize salience at the skin. Chapter 3 presents the studies I performed to determine how well people can respond to a vibrotactile system. Chapter 4 focuses on the method I developed to study perception localization on the lower limb. Chapter 5 introduces Targeted Reinnervation and how it can be leveraged to provide natural feedback for the lower limb. Chapter 6 concludes this dissertation by discussing how this work can be utilized to inform future designs of a vibrotactile sensory feedback system for lower limb prostheses.

Chapter 2. ACTUATORS FOR SENSORY FEEDBACK

2.1 BACKGROUND

2.1.1 *The Somatosensory System*

The nervous system consists of a network of neurons that communicate between the peripheral nervous system (PNS) and the central nervous system (CNS). Efferent nerves communicate motor controls from the CNS to the muscles, and afferent nerves convey sensory information from the PNS back to the CNS. Sensory receptors initiate nerve impulses, sensation occurs when nerve impulses arrive at the cerebral cortex of the brain, and perception is what the cerebral cortex interprets the meaning of those sensations to be [41]. Our fast-working feedback system is integral to how we interact with and react to our environment.

All of the sensations we perceive are transmitted through action potentials fired by special classes of sensory receptor neurons. There are 13 known receptors: 4 types of cutaneous mechanoreceptors, 2 types of pain receptors, 2 types of temperature receptors, 1 type of itch receptor, and 4 types of receptors located in the muscles, tendons, and joints for proprioception and body movement [42]. Information obtained by the receptors is communicated through characteristic streams of action potentials that reach the spinal cord and eventually the cortex [42].

We rely on mechanoreceptors for all of our touch sensations, such as feeling textures, grooves, and pressures. They are classified as slowly adapting (SA) or rapidly/fast adapting (RA or FA) based on how they respond to sustained pressure on the skin [43]. They can also be classified into types by the size of their receptive fields. Small receptive fields (type I) tend to give higher resolution sensations while large receptive fields (type II) will trigger sensations in a general area [44]. Additionally, they can be classified by the axon fiber type which determines how quickly electrical impulses can be conducted. Axons with thinner diameters conduct signals slower than large diameters, and myelination of the axon also helps to quicken signal conduction [45].

In order for them to be most effective, these receptors generally reside in the layers of the skin as shown in Figure 2.1 [46]. Merkel disks and Meissner corpuscles are the closest to the surface, right blow the epidermis at the apex of dermal papillae. Ruffini corpuscles exist in the dermis and hypodermis while Pacinian corpuscles reside solely in the hypodermis [47]. Ruffini corpuscles can also be found in joint capsules and special mechanoreceptors are also found in the musculature

that can detect tension in the muscle [42]. These receptors are classified as proprioceptors, which are important for conveying information about the position of your body in space and contribute to balance [48]. Proprioceptors include muscle spindles, golgi tendon organs, and joint receptors [48].

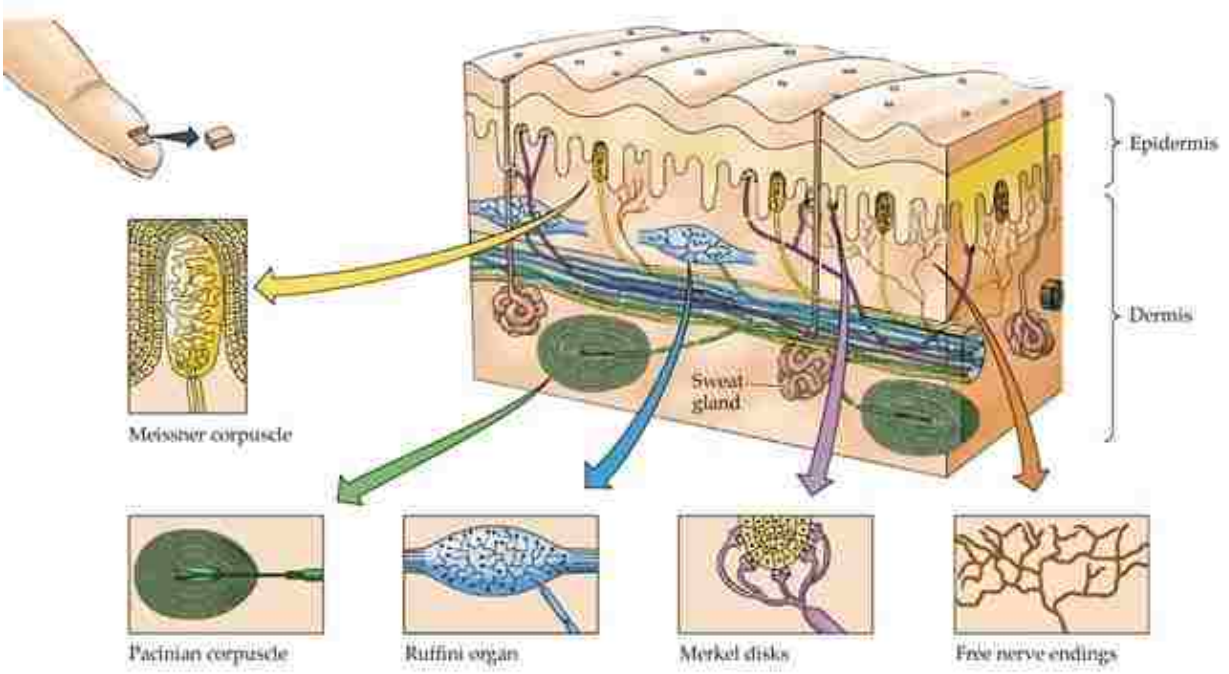

Figure 2.1 – Location of mechanoreceptors in the skin [140].

Vibrations are generally picked up by the Pacinian corpuscles (RA type II) that are oval-cylindrical shaped and 1mm in length. These mechanoreceptors are sensitive to vibrations in the range of 250-350 Hz and great for detecting gross pressure changes [49], [50]. However, since they are rapidly adapting, continual stimulation will cause the mechanoreceptors to adapt and tune out the signal. Touch and pressure tend to activate the Merkel disk (SA type I). They are slowly adapting, thus have a sustained response to pressure and modulate the speed at which they fire depending on the curvature of indentation (fastest for small points and slow for large curves or flat surfaces) [51]. Merkel nerve endings are extremely sensitive and could be triggered by displacements less than 1μm [51].

Resolution of multiple points of perception is both a property of the mechanoreceptor structure (size/mechanical properties) and its density in a particular area of the body. Vibration on the skin of the arm 2cm apart may be sensed differently than pressure at those same spots due to the different mechanoreceptor structures that detect each of those sensations. Additionally, our

hands are much better at distinguishing touch sensations than our thighs even though they contain similar types of mechanoreceptors because the hands contain the largest density of mechanoreceptors while the thigh does not. The 2-point discrimination test (Figure 2.2) is what is most commonly used to determine receptor density and difference sensitivity at different areas of the skin. This test stimulates an area of skin with two points that are close together and slowly moved apart. When the two points are very close, people will report that they feel only one point because they are stimulating within the receptive field of one mechanoreceptor. As the points are moved apart, multiple mechanoreceptors are stimulated and people will report feeling two points instead of one [41].

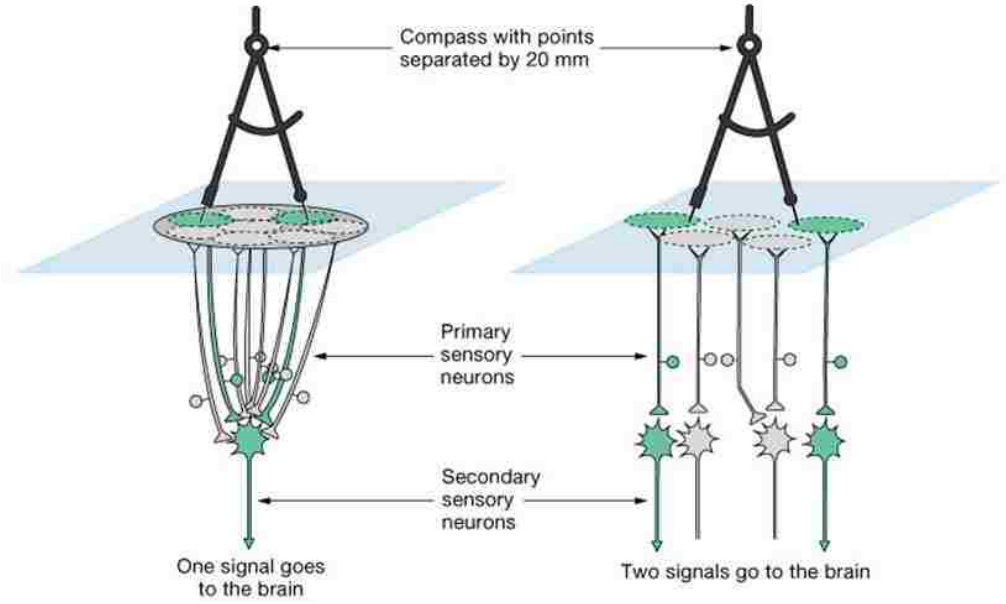

Figure 2.2 – Two-point discrimination test. Left: Large receptive field where only one sensory neuron is stimulated so two points will be perceived as one. Right: Small receptive field where only a few neurons are associated with one sensory neuron so two points will be perceived.

After mechanoreceptors pick up sensation, they conduct the signal to the somatosensory cortex of the brain, which allows people to *perceive* sensations. Perception is how our brains interpret sensation by attaching meaning or feeling or thought to it. Figure 2.3 shows the primary somatosensory cortex (S1) with specific body parts oriented above their representative locations.

Larger areas of the S1 are dedicated to areas that typically have more sensory receptors and therefore need more processing power from the cortex.

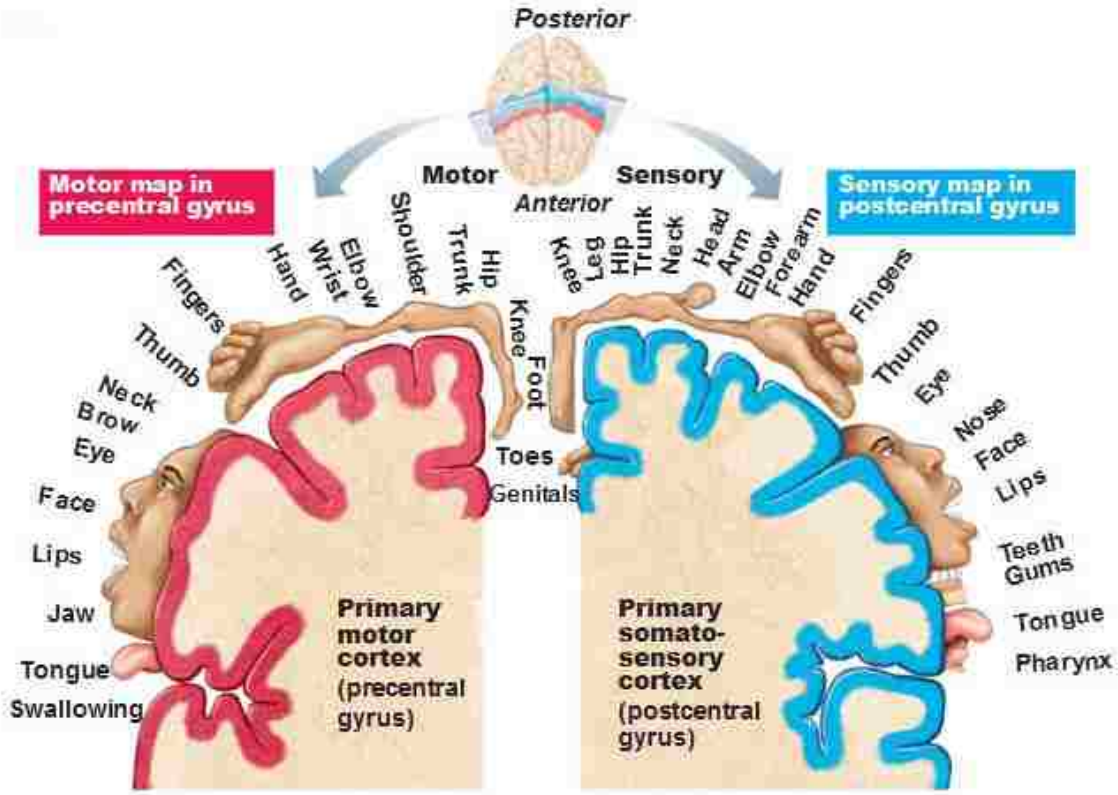

Figure 2.3 – The sensory and motor homunculus [141].

2.1.2 *Choosing an Actuator*

Vibration motors tend to be small, lightweight, power efficient, and low-cost as a result of the popular cell phone market. The most common types of actuators are linear resonance actuators (LRAs) and eccentric rotating mass motors (ERMs). LRAs operate by oscillating a magnetic field to vibrate a magnet connected to the case by a spring and require an AC input. They typically have one resonant frequency at which they operate and are directional. ERMs are DC motors that have an offset mass rotating about the center axis. The non-symmetric rotating mass causes displacement of the motor body at high frequencies to produce vibration. Frequency and amplitude of ERMs are coupled, which means that an increase in frequency (directly proportional to voltage) typically causes a linear increase in amplitude of vibration. Engineering Acoustics Inc. (Casselberry, Florida) has developed proprietary LRAs (C-2 and C-3 tactors) that minimize size,

weight, and power consumption. Additionally, these tactors have drivers that can separately modulate amplitude and frequency, allowing for more complex vibration sensations. ViviTouch has created its own type of actuator using electroactive polymers (EAP) that are extremely thin, have a 4x faster response, and uses up to 70% less energy [52]. Similarly, these EAP devices can be separately modulated in both amplitude and frequency.

A method of providing mechanical pressure was also studied since there are possible differences in sensation/perception capabilities between vibration and pressure. Fan was the only researcher that studied a pressure sensation instead of vibration on the leg. He used a pneumatic system to inflate/deflate balloons that were held against the thigh [35], [36]. However, a pneumatic system is slow (mechanical lag to inflate the balloon) and not portable (subjects must be directly connected to pneumatic actuators). I tested small 5V solenoids (Sparkfun, CO), but they did not produce enough force and had to be positioned at a very specific height above the skin in order to exert maximum force. Since I was not able to design a mechanical system that could mechanically exert pressure that was portable and salient enough to be felt on the thigh, only vibration actuators were tested in my studies.

Based on the extensive use of vibrotactile actuators in literature, low cost, small form factor, and quick response time, we decided to test both LRAs and ERMs as the feedback actuator for our system. In order to secure these motors against the thigh, we designed a housing that held the motor to the thigh via an elastic band. However, due to lower sensation in the thigh compared to other parts of the body [53], [54], initial tests resulted in nearly imperceptible stimulation. We think a large contributing factor was our block design, which couples the vibrating motor with the damping of the elastic band and skin. In this chapter, we analyze and simulate the mechanical system in order to design a more efficient holder that maximized the amount of skin displacement without additional energy input.

Accurately modeling this interface requires understanding of skin mechanics. Skin can be approximately described as a viscoelastic mechanical system [55]. When in contact with a mechanical interface, there is an effective impedance presented by the skin to the mechanical device [56]. Skin's mechanical impedance depends on contact area [57], location on the body [58], frequency [59], and indentation [60]. All of these variables have a complex interaction and affect skin elasticity in a nonlinear pattern [61]. We will use the skin model described in Lindsay's [62] paper as he accounts for the same parameters we are interested in.

Mechanical systems like our vibrotactile actuators have a resonant frequency at which they vibrate most efficiently [63]. At this frequency, mechanical impedance is low and little energy is required for the whole system to vibrate at a large amplitude [58]. By placing the actuator in a suspension system tuned to its resonant frequency, we hope to increase the amplitude of vibration. In addition, we have decoupled the vibrating mass from the elastic band in order to more efficiently transfer vibration energy from the actuator to the skin.

Using our mechanical model and numerical optimization, we designed new holders for both LRAs and ERMs that increased skin displacement. This chapter will describe the new design, engineering optimization, and test results for the new and initial holder prototypes.

2.2 Initial Design Model

Two basic holders, which we will call the block design, were 3D printed (Dimension bst 768, Stratasys, MN) in acrylonitrile butadiene styrene (ABS) plastic (Figure 2.4. – Original block holders mounted on a purple elastic band. (Left) Block LRA holder, (Right) Block ERM holder.). The design goal was to hold the vibrational actuators comfortably against the skin without blocking their motion.

Figure 2.4. – Original block holders mounted on a purple elastic band. (Left) Block LRA holder, (Right) Block ERM holder.

A mechanical model of each system was designed using the standard system diagram approach (Figure 2.5). In our system, the vibrational actuator has a rigid connection to the block holder, which is held in contact with the skin by an elastic band. The models of the actuators were

created by direct analysis of the C10-100 LRA and a Pico Vibe 307-002 (Precision Microdrives, London, UK).

M_{att} is the mass of the holder in rigid contact with the vibrating motor, which is held by an elastic band with properties K_{ba} and B_{ba} against the skin, described by K_s and B_s.

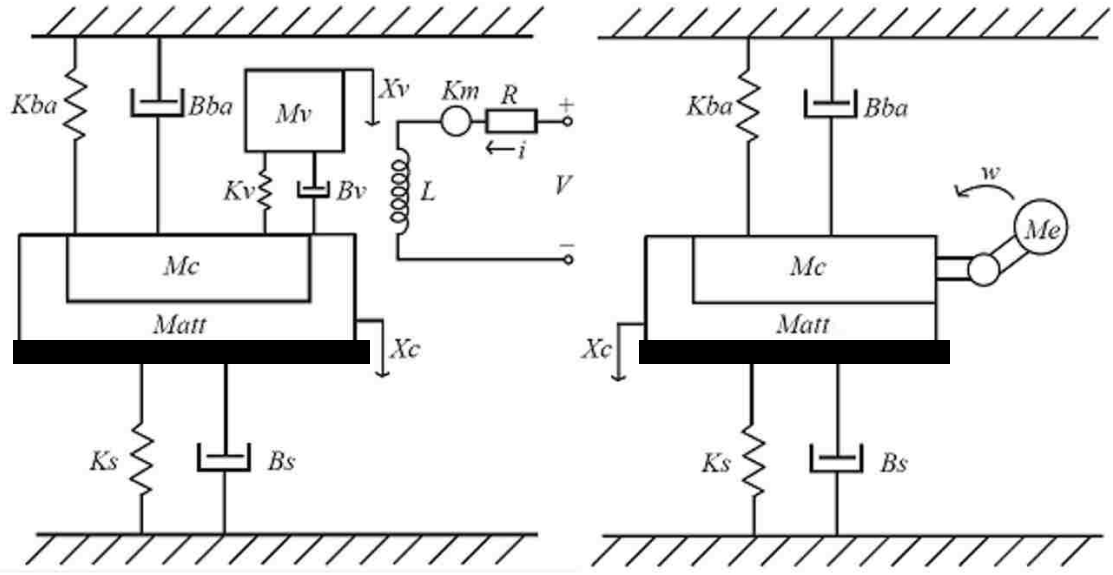

Figure 2.5. – LRA (left) and ERM (right) mechanical models of Block designs applied to skin. The bold surface denotes *A.*

The model for the LRA system can be described by the following equations of motion:

$$Li + iR + K_m(\dot{x}_c - \dot{x}_v) = V \tag{2.1}$$

$$M_v\ddot{x}_v + B_v(\dot{x}_v - \dot{x}_c) + K_v(x_v - x_c) = -K_m i \tag{2.2}$$

$$M_t\ddot{x}_c + B_v(\dot{x}_c - \dot{x}_v) + K_v(x_c - x_v) + (B_s - B_{ba})\dot{x}_c + (K_s + K_{ba})x_c = 0 \tag{2.3}$$

$$M_t = M_c + M_{att} \tag{2.4}$$

The model for the ERM system can be described by the following equation of motion:

$$M_t\ddot{x}_c + (B_s + B_h)\dot{x}_c + (K_s + K_h)x_c = M_e r\omega^2 \sin(\omega t) \tag{2.5}$$

For each device we can transform the equations of motion into the form $\dot{x} = Ax + Bu$. The csim() utility in Scilab [64] was used to simulate the time response of this system to sinusoidal inputs. The input to the LRA (V) had an amplitude of 5V (10V peak-to-peak) and a frequency of 175 Hz. The input to the ERM (ω) was 942 rad/sec. Modeling perception is beyond the scope of this thesis. Instead, our proxy for vibrotactile sensation is skin displacement (x_s) which is represented by peak displacement values.

Parameter values (Table 2.1, Table 2.2, Table 2.3) were taken from datasheets, measured in the lab, or taken from related literature. Masses were found by weighing the components after disassembly. The elasticity, damping, and motor constant of the LRA and elasticity and damping of the skin were taken from previous work by Lindsay [62]. The band is made from 3mm thick neoprene and its spring and damping properties were calculated by measuring its oscillation frequency and relaxation time constant when loaded with a known mass and allowed to oscillate.

Table 2.1 – Common model parameters

Parameter	Description	Value	Source
K_S	Skin Elast.	600-1200 *N/m*	[62]
B_s	Skin Damp.	0.75-2.38 *Nsec/m*	[62]
K_{ba}	Band Elast.	16 *N/m*	Measured
B_{ba}	Band Damp.	14 *Nsec/m*	Measured

Table 2.2 – LRA model parameters

Parameter	Description	Value	Source
L	Inductance	130μH	Datasheet
R	Resistance	28Ω	Datasheet
M_v	Moving Mass	1.4g	Measured
M_c	Case Mass	0.6g	Measured
K_v	LRA Elast.	2800 *N/m*	[62]
B_v	LRA Damp.	0.0322 *Nsec/m*	[62]
K_m	Motor Const.	1	[62]
M_{att}	Holder Mass	2.3g	Measured

Table 2.3 – ERM model parameters

Parameter	Description	Value	Source
M_e	Eccentric Mass	$1.7g$	Measured
r	Radius of Rotation	$1.43mm$	Calculated
M_c	Case Mass	$1.2g$	Measured
M_{att}	Holder Mass	$4.8g$	Measured

2.3 New Design Model

Our original LRA attached to a block holder elicited a very weak sensation when applied to the thigh. Based on our insight that the actuator needed to be decoupled from the strap and body, we designed a new device for both the LRA and ERM that suspended the motor in the middle of the holder via elastic bands characterized by a spring constant of vertical displacement K_h. This new design (Figure 2.6 and Figure 2.7) also serves to decrease the mass (M_{att}) that the motor must vibrate and therefore increase the energy devoted to skin displacement.

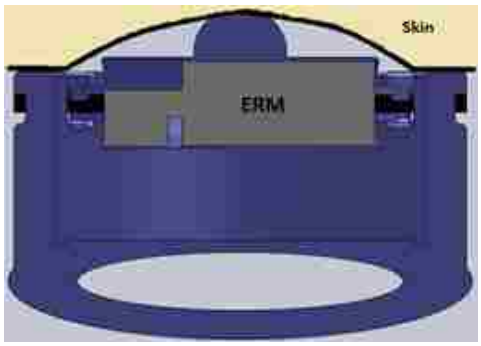

Figure 2.6 – Cross section of Solidworks model of new suspended design. Black represents the silicone suspension system that holds the moving mass in the center.

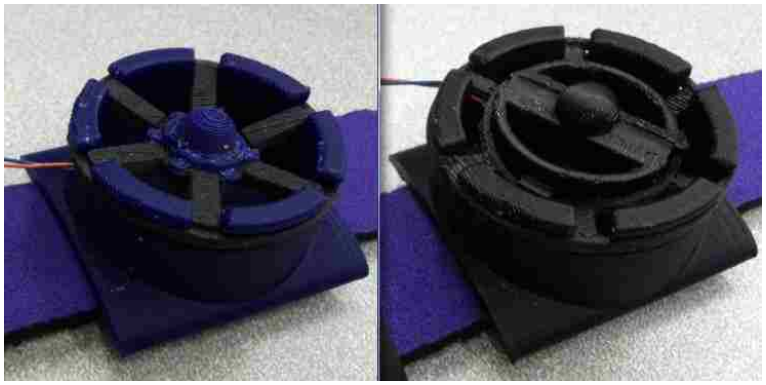

Figure 2.7 – LRA (left) and ERM (right) suspension designs.

Our suspension system used silicone (Permatex, Hartford, CT) that was molded into a six-spoke ring that suspended the moving mass in the center of the holder. The dimensions of each spoke were calculated using Young's modulus (average of 3Mpa) to produce the desired K_h found by our optimization. The molds were printed with a 3D printer, filled with silicone, left to cure over 48 hours, and finally the silicone was removed (Figure 2.8).

Figure 2.8 – Optimized silicone suspension systems for new LRA (left) and ERM (right) design.

In order to optimize K_h, we used a mechanical model for this suspension system and solved for the K_h value to maximize skin displacement (Figure 2.9).

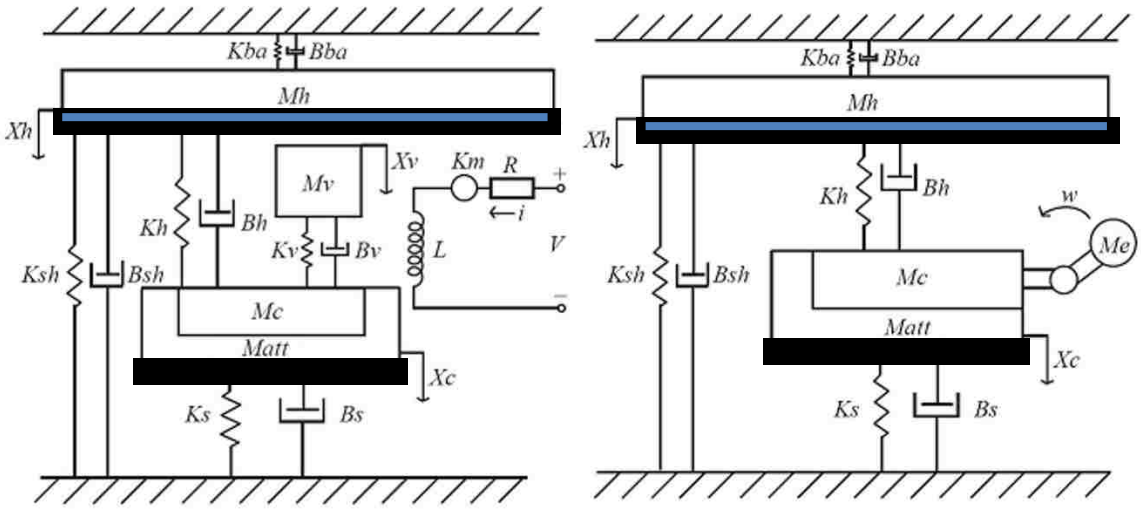

Figure 2.9 – LRA (left) and ERM (right) mechanical models of new suspension housing designs applied to skin. The bold black line denotes A and the bold blue line denotes A_h.

The model for the LRA system can be described by the following equations of motion:

$$Li + iR + K_m(\dot{x}_c - \dot{x}_v) = V \quad (2.6)$$

$$M_v\ddot{x}_v + B_v(\dot{x}_v - \dot{x}_c) + K_v(x_v - x_c) = -K_m i \quad (2.7)$$

$$M_t\ddot{x}_c + B_v(\dot{x}_c - \dot{x}_v) + K_v(x_c - x_v) + B_s\dot{x}_c + K_s x_c + B_h(\dot{x}_c - \dot{x}_h) + K_h(x_c - x_h) = K_m i \quad (2.8)$$

$$M_h\ddot{x}_h + B_h(\dot{x}_h - \dot{x}_c) + K_h(x_h - x_c) + (B_{ba} + B_{sh})\dot{x}_h + (K_{ba} + K_{sh})x_h = 0 \quad (2.9)$$

The model for the ERM system can be described by the following equations of motion:

$$M_t\ddot{x}_c + B_s\dot{x}_c + K_s x_c + B_h(\dot{x}_c - \dot{x}_h) + K_h(x_c - x_h) = M_e r\omega^2 \sin(\omega t) \quad (2.10)$$

$$M_h\ddot{x}_h + (B_{ba} + B_{sh})\dot{x}_h + (K_{ba} + K_{sh})x_h + B_h(\dot{x}_h - \dot{x}_c) + K_h(x_h - x_c) = 0 \quad (2.11)$$

2.3.1 *Optimization of Suspended Design*

Using the new suspended model, we began to study the effects of each parameter on skin displacement. Initial simulations showed that varying the contact area between the device and the skin (A_h), the mass that holds the motors (M_{att}), and spring constant (K_{ba}) had a large effect on skin displacement (x_s).

A brute force numerical search was performed over 6 parameters (K_h, B_h, A_h, A, M_{att}, M_h) to maximize skin displacement (Table 2.4). The search bounds for K_h and B_h were set at 10^{-3} and 10^3 with exponentially increasing increment values. The search bounds for A_h and A were set at 10^0 and 10^3, also incremented exponentially. The search bound for M_{att} was set at 0.1 and 10.0g and incremented at intervals of 0.1. The search bound for M_h was set at 0.1 and 50.0g and incremented at intervals of 0.1. We arrived at these search bounds because they were within the size constraints of the system and we knew they would encompass optimal values based on some rudimentary calculations. After searching through a large range, we refined our search range around initial results. The optimization for ERM and LRA designs were performed separately.

Table 2.4 – Parameter search ranges and number of values within the range that was searched.

Parameter	Description	# Values	Search Range
K_h	Holder Elasticity	133	$10^{-3} – 10^{3}$ *N/m*
B_h	Holder Damping	82	10^{-3}–10^{3}*Nsec/m*
A_h	Contact Area (holder)	46	$10^{0} – 10^{3}$ mm^2
A	Contact Area (moving mass)	46	$10^{0} – 10^{3}$ mm^2
M_{att}	Mass attached to motor	100	0-10*g*
M_h	Mass of holder	500	0.1-50*g*

The results of the numerical search for the two new suspension devices yielded parameter values which maximized skin displacement (Table 2.5). The new devices were then simulated using these optimized parameter values and results are shown by the blue lines while the old design simulations are shown in red (Figure 2.10). Maximum displacement values are shown in Table 2.6.

Table 2.5 – Optimal parameter values used in new devices.

Parameter	Optimal Value (LRA)	Optimal Value (ERM)
K_h	1700 *N/m*	2200 *N/m*
B_h	0.001 *Nsec/m*	0.001 *Nsec/m*
A_h	306 mm^2	306 mm^2
A	314 mm^2	314 mm^2
M_{att}	0.3*g*	1.2*g*
M_h	10.2*g*	10.9*g*

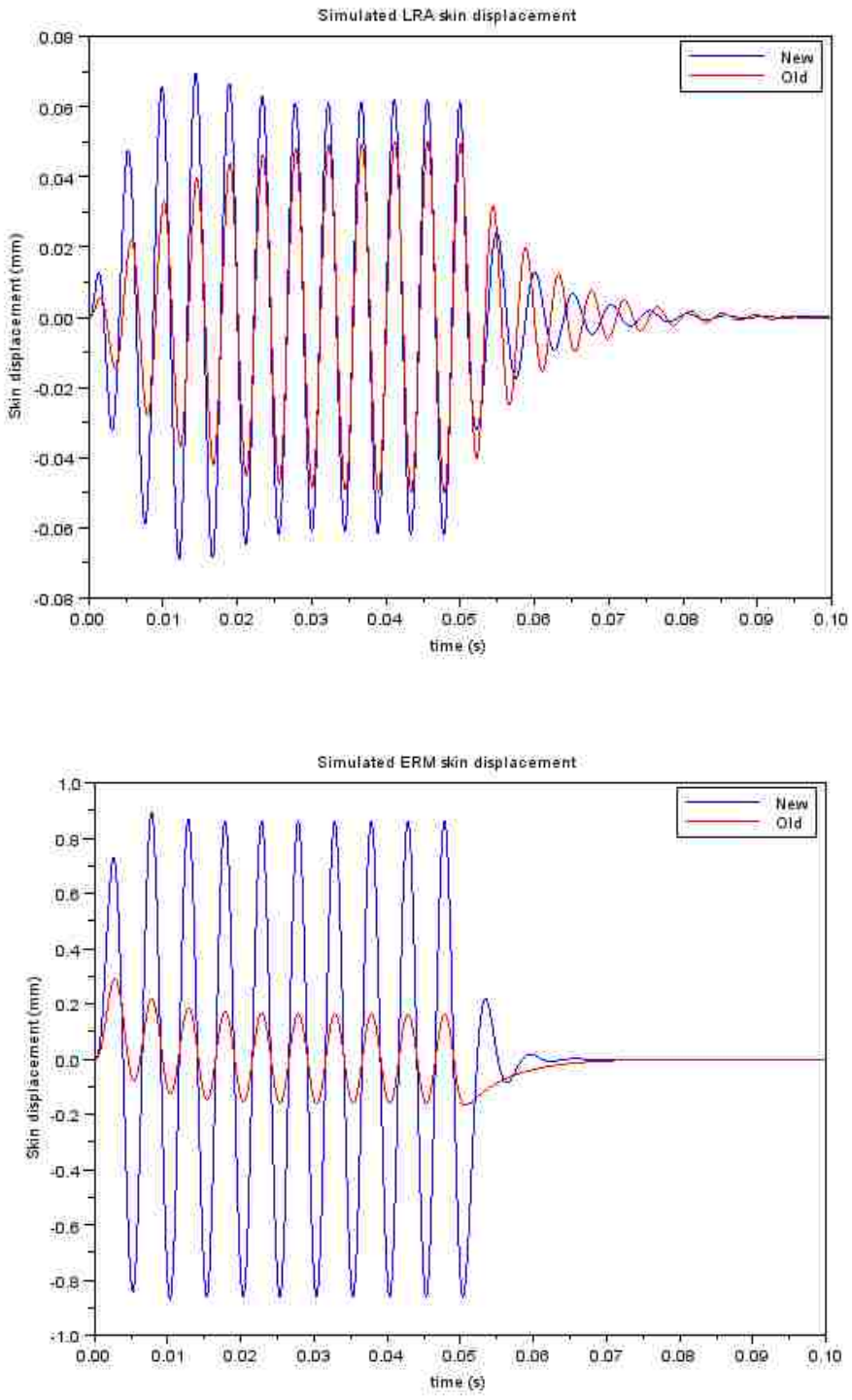

Figure 2.10 – Simulated skin displacement. Top: LRA block (red) vs suspension (blue) design. Bottom: ERM block (red) vs suspension (blue).

*Note the different scales on the y-axis.

The results of the simulation show that maximum skin displacement of the new LRA holders are 0.07mm compared to 0.05mm for the block design. A larger difference can be seen in the new ERM holder, which results in 0.9mm of skin displacement compared to 0.3mm.

2.4 Displacement Test

2.4.1 *Method*

In order to quantify the improvement using our optimized holder, we performed a displacement test while the motor was held against the skin of the thigh. A laser sensor (Keyence, NJ; model IL-030) and amplifier (Keyence IL-1000) was used to measure displacement of the moving mass against the skin. We assumed the moving mass stays in contact with the skin as it vibrates, thus we can infer skin displacement. Data from the laser was read with an oscilloscope (Tektronix TDS3032).

Laser sensor calibration was 1mV per 1µm of displacement. This was verified by shining the laser on a desk and then sliding a washer of .3mm thickness underneath the laser to confirm correct voltage change (300mV). The laser was firmly secured in a position above the vibrating device within the device's measurement rage of 20-45mm.

The holders were printed using a 3D printer (Figure 2.5 and Figure 2.7). Holes were drilled in the back of the suspended designs to allow the laser to measure the movement of the moving mass. A piece of white cardstock paper was hot glued to the measured surface to provide better reflection for the laser. The housings were connected to an elastic band through the loop hole, and the elastic band held the device against the skin on the thigh during the data collection.

The LRAs were driven with a square wave, ±5V at 175 Hz. The ERMs were driven with a DC power supply at 1.5 V.

2.4.2 *Results*

Displacement data from the laser sensor was collected with an oscilloscope (Figure 2.11 and Figure 2.12). Amplitudes were estimated from the oscilloscope readouts and converted to distance at the ratio of 1mV to 1μm. Maximum displacement was taken to be half of the peak-to-peak amplitude to stay consistent with our simulations that describe the motor oscillating about the surface of the skin, which is zero displacement.

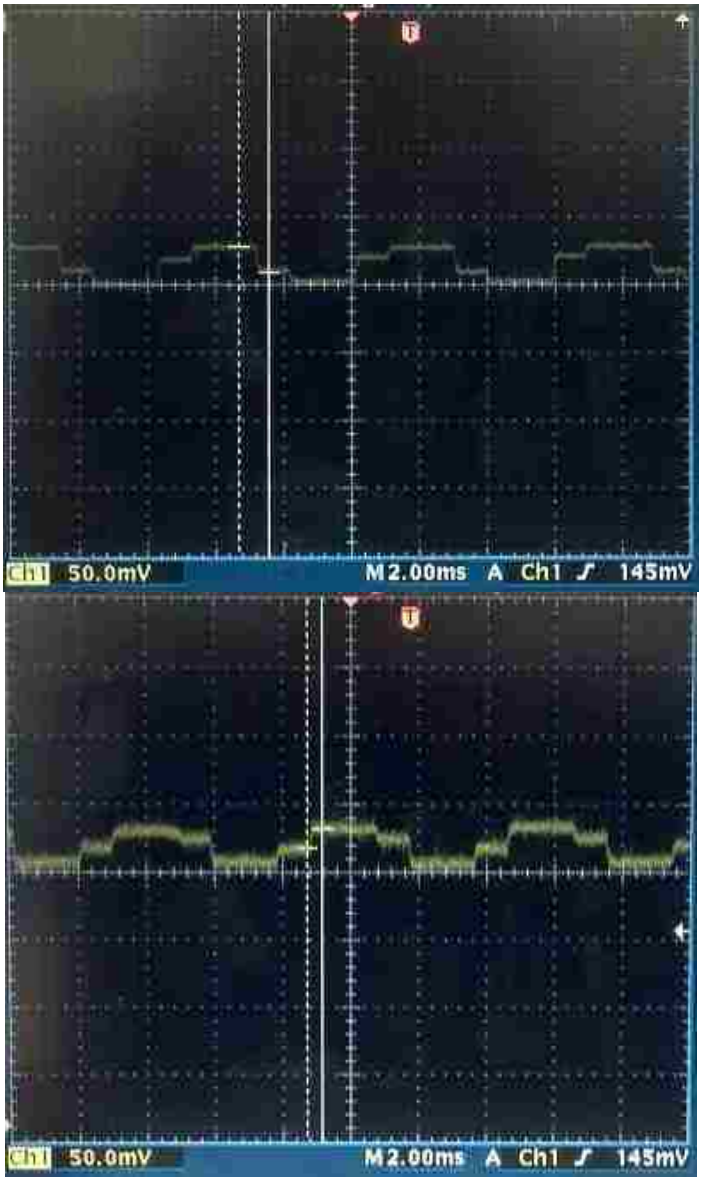

Figure 2.11 – Meaured skin displacement for LRA devices. Top: Block design. Bottom: Suspension design. *Note the different scales between Figure 2.11 and Figure 2.12.

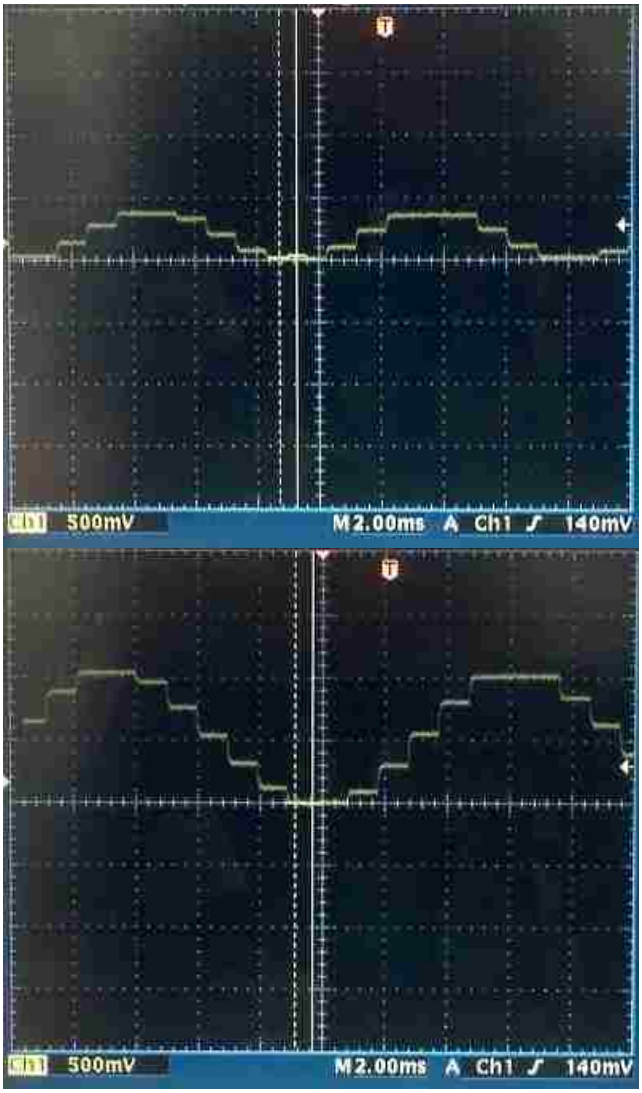

Figure 2.12 – Measured skin displacement for ERM devices. Top: Block design. Bottom: Suspension design. *Note the different scales between Figure 2.11 and Figure 2.12.

Table 2.6 – Maximum displacement values (mm)

	Old Design		**New Design**	
	Simulated	**Measured**	**Simulated**	**Measured**
LRA(max)	0.0506	0.015	0.0696	0.018
ERM(max)	0.291	0.19	0.892	0.5

2.5 DISCUSSION

We have described simulation, prototyping, and data collection experiments to study vibrotactile holder modifications towards optimization of skin displacement. We studied two actuator types (LRA and ERM) and two mounting systems. Our results focus on skin displacement, which we assume correlates with perception.

Maximum displacement of the suspended LRA increased by a factor of 1.38 in the simulation and by a factor of 1.2 when measured. The simulation of the LRA models and the actual measured values are similar, with the new LRA design only slightly increasing the displacement.

For the ERM based design, maximum displacement increased by a factor of 3.07 in the simulation and increased by a factor of 2.63 when measured. The simulation and measured results show similar improvement with the suspended design.

Both types of motors showed some improvement using the suspended design, but the absolute displacement values do not agree. The old LRA design was measured to displace 0.035mm less than the simulation, and the new LRA design was measured to be 0.0516mm less. Similarly, there was disparity for the ERM design as well, with the old design measuring 0.1mm less than simulated and the new design measuring 0.392mm less.

This discrepancy could be explained by inaccuracies in our skin model, which assumes zero displacement when the motor sits on the skin. It is more likely that there is some initial depression, and the displacement measure most relevant to perception would be a factor between 0.5 and 1.0 times the peak-to-peak amplitude.

In this work, we focus on skin displacement, but in actuality, human perception of vibration is correlated with more than skin displacement. Future work will test these devices on human subjects in order to determine actual perception instead of just skin displacement. Using our method for measuring skin displacement, we may be able to quantify the correlation between skin displacement and perception.

This chapter demonstrates the ability to increase skin displacement of a vibrotactile actuator by optimizing holder design. Simulations of the new suspended optimized designs showed marked improvement in skin displacement over the old block designs. Data collected with a laser sensor show a similar factor of increase between the two LRA designs. However, the difference in skin displacement between simulated and measured values suggest other factors may be at play.

Validation of a more effective holder ultimately lies in testing human subjects for perception as well as skin displacement.

Chapter 3. CHARACTERIZATION OF HUMAN RESPONSE TO VIBROTACTILE FEEDBACK

3.1 BACKGROUND

3.1.1 *Human Reaction time*

Reaction to a stimulus is comprised of the time it takes to activate the sensory neuron, travel to the cortex, travel to the motor neuron, and activate the motor neuron to contract the muscle fibers. The speed of transmission depends on the type of nerve, its axon diameter, its length, and whether or not it is mylenated. Due to these factors, neurons from different sources have inherently different impulse speeds (Muscles: 119 m/s, touch: 76.2 m/s, pain: 0.61 m/s) [45]. Different types of sensory stimuli also exhibit different speeds because of their proximity to the cortex. Auditory stimulus takes 8-10ms to reach the brain and visual stimulus takes 20-40ms [65], [66]. Reaction time for auditory stimulus is 140-160ms, visual is 180-200ms, and touch is 155ms [65]–[67]. Differences in reaction time tend to persist within the same subject whether the response is simple or complex, and between different sensory stimuli [68]. The speed of reaction is primarily affected by the cognitive response time [69]. Reactions could be categorized into simple (220ms, recognition (384ms), and choice (proportional to number of choices – Hick's Law), each of which are cognitively more challenging and therefore have respectively longer reaction times [70]–[77]. People can train themselves through repetition to respond faster by reducing the cortical load, thus minimizing response time to mostly travel time.

Reflexes are fast because they circumvent the need for a stimulus to travel to the cortex before triggering a muscle reaction. Depending on the reflex/reaction that is stimulated, either a monosynaptic or polysynaptic response is triggered. Monosynaptic responses are very fast and result only in one muscle activation. A polysynaptic response will recruit multiple muscle groups that work together in order to achieve a response. A trip reaction has been shown to trigger a polysynaptic reflex because there are multiple muscles that work together to achieve balance and posture [78], [79]. After the onset of a trip, Pijnapples found that some of the first muscles to respond (fastest reaction time) were from the support limb and not the swing limb [80], [81].

Table 1
Onset times (and SD) of muscle responses after tripping in the support limb (contralateral) and swing limb (ipsilateral), averaged over subjects

	Tripping			
	Support limb		Swing limb	
Gluteus maximus (GL)	79	(8)	82	(15)
Biceps femoris (BF)	65	(7)	90	(18)
Semitendinosus (ST)	63	(4)	86	(18)
Rectus femoris (RF)	136	(38)	104	(38)
Vastus lateralis (VL)	96	(22)	115	(25)
Tibialis anterior (TA)			76	(8)
Gastrocnemius medialis (GM)	71	(12)	119	(12)
Soleus (SO)	73	(9)	101	(14)

In TA of the support limb, no responses could be detected within 200 ms after impact.

Figure 3.1 – Table from [81] showing the muscle response time after tripping.

Figure 3.1 shows that much of the muscle response occurs within the first 100ms of tripping. There is a very small window in which people can prevent a fall once tripped, and it is possible that amputees suffer from a delay in this feedback. The lack of limb and its associated mechanoreceptors means that amputees may not receive information about a trip until it is too late to respond.

3.1.2 *How People Fall*

For our lower limb prosthesis feedback system, we are interested to see if we can send information to warn amputees about falls. Most fall studies have focused on the elderly and normal population, but not much work has been done to determine underlying mechanisms of falls and successful balance recovery in lower limb amputees. To the best of our knowledge, the only study found on falls in amputees was Curtze's paper on balance recovery after an evoked forward fall [82]. In this study, they used a tether-release technique (Figure 3.2) that requires subjects to recover balance after being suddenly released from a forward-inclined orientation that supported 10% of their body weight. Two force plates were used to measure the ground reaction forces and full-body kinematics were captured by an eight-camera Vicon motion capture system and 35 reflective markers. Response time was measured in milliseconds (ms) and defined as the time between release and toe-off of the leading limb. All participants were able to recover except one amputee who slipped after being released. Surprisingly, Curtze found that amputees responded statistically significantly faster than controls (219.5 ms vs. 239 ms) [82]. However, their experimental set up

does not adequately address the response to an unexpected trip caused by a perturbation to the prosthetic leg. The tether-release technique does not simulate a real-life situation to which people must respond. Suspension from the torso provides the same amount of sensory, vestibular, and visual feedback for both subject groups, so it is possible that amputees can still respond as quickly as non-amputees if they know a fall is happening.

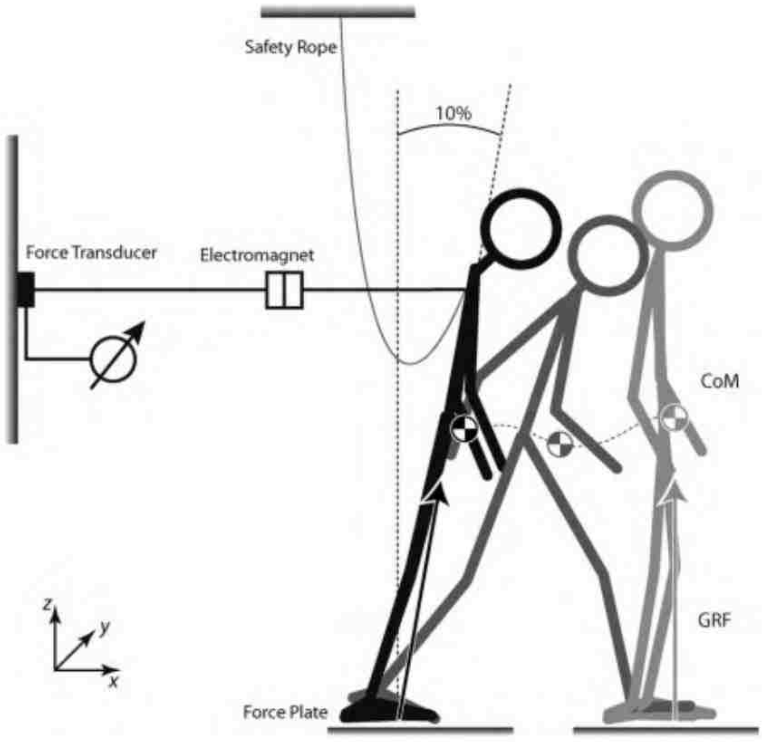

Figure 3.2 – Tether release technique from [82].

Based on Curtze's study using a tether and motion cameras, an amputee would require roughly 219ms to initiate a corrective step [82]. However, feedback systems that have been researched in the past show reaction times (RT) that are much slower than this. Wentink's experiment tested auditory and electrotactile feedback on the thigh while subjects walked with a fake prosthetic leg on a treadmill [33]. She found that auditory feedback (RT 240ms) was significantly different than electrotactile (RT 270ms) by 30-40ms [33]. Asseman's experiment had amputees standing still on a platform that was unpredictably accelerated to cause a trip, and a warning vibration was provided to the forehead (RT 281ms) or back of the head (RT 273ms) to respectively cue either a forward or backward stepping response [31], [32]. Sharma performed a comprehensive study on

vibrotactile feedback and found that when a stimulus was applied to the leg, a hand-pushed response button (RT 568ms) elicited a faster response than a leg-pushed response button (RT 712ms), and that the anterior position (RT 599ms) had the fastest RT compared to the other three sides [39]. Sharma's experiments provide a good benchmark for vibrotactile feedback on the thigh, but since these experiments were done while sitting, it is unclear if similar RTs are expected while walking.

3.1.3 *Vibration as Feedback*

Vibration is a practical and widely adopted means of feedback, especially while visual concentration is elsewhere. This is why vibrational feedback has been used in a variety of devices such as game controllers, cell phones, and pagers. The prosthetic DEKA arm uses a vibrating motor applied to the residual limb that changes in intensity relative to how hard the fingers are pressing on an object [83]. Army Research Laboratory built vibration motors into a shirt paired with a glove with sensors for military tactical use [84]. They created a vocabulary using vibration pulses that could be learned in a couple hours, so while wearing the shirt in the field and out of direct sight, soldiers could still silently communicate with each other. This has promising implications for a vibrotactile system designed to communicate non-urgent messages to a user, such as lack of socket stability due to fluid loss in the limb. Most notably, many car companies are looking at using vibration as a means to warn drivers they are too close to the car in front and should brake. Studies have shown that between visual, auditory, and vibrotactile feedback, drivers who received the vibration warning had the shortest response time [85].

Feedback useful to fall prevention must be delivered while walking. We surmise that walking puts extra burdens on tactile senses (vibration from when feet hit the ground and muscle contraction) and visual senses (scanning the environment and path planning), potentially increasing RT [86], [87]. To the best of our knowledge, no paper has compared more than two types of feedback modalities or shown how walking affects RT. It may also be important to signal different types of responses for different types of trip situations, further increasing human reaction time.

In order to determine whether or not our system is suited to provide trip feedback, this chapter will study human reaction time and ability to differentiate between multiple motors while walking. It is important to understand the limitations of human interactions with different feedback

modalities, which can inform future design choices when developing sensory feedback for prosthetic legs.

3.2 Reaction Time While Walking

The purpose of this study was to measure reaction time to stimuli relevant to lower limb prosthetic feedback, and provide a comparison of sensory feedback modalities while a person is walking versus standing. We tested six different sensory modalities: visual, auditory, vibration on wrist, vibration on waist, vibration on thigh, and vibration on toe.

Figure 3.3 – Testing device and placement: Glasses frames with LED and headphones on the head, vibrotactile motors (located at the 4 red boxes), electronics pack held in the non-dominant hand, and response buttons held in the dominant hand.

The testing device (Figure 3.3) consisted of five units: an electronics pack, glasses frame with an LED (no lenses), headphones, a vibrotactile unit that can be secured over the four tested areas

with an elastic band, and a hand held response button. The electronics pack contained an Arduino Mega 2560 microcontroller board that logs reaction time information on a MicroSD card breakout board (Adafruit, New York). Visual stimulus was provided by an orange LED mounted to the top right corner of an empty glasses frame. A 262 Hz auditory stimulus was given through non-noise-cancelling headphones (Audio-Technica ATH-M20) at about 70 decibels. Vibrotactile feedback was given by an Eccentric Rotating Mass (ERM) motor (Precision Microdrives, London, UK) mounted in the suspension holder described in Chapter 2. Vibration of the motor could not be heard, so no additional actions were taken to mute the noise. Mechanical delay of the vibration motor on skin was tested by an IL-030 analog laser sensor (Keyence, Itasca Il.) and measured with an oscilloscope (Tektronix TDS 30320). A 46ms lag was detected between ERM actuation signal and laser-measured skin displacement. Lag from the microcontroller processes (software detecting button press and storing the data) was not measured as it should be negligible.

3.2.1 *Method*

12 non-disabled participants with an average age of 27 years (SD 3 years, 7 male/5 female) were recruited for this study. All of the participants were recruited at the University of Washington and had no known sensorimotor deficits. The study was approved by the University of Washington Human Subjects Division (Study #44011).

Participants were told that the purpose of the test was to measure reaction time and that accuracy would be taken into account. Participants were fitted with the test devices one at a time so that unused objects would not distract them during the trial. Stimuli were applied to the dominant side, defined by the handedness of the participant. The LED was always mounted on the top right corner of the glasses frames, but all tested participants in this study were right-handed. Participants responded by clicking a button that was held in their dominant hand while the other hand carried the electronics that actuated the stimuli and logged all reaction times.

Each trial consisted of 25 stimuli and nulls that each lasted 1000ms. Delay between each stimulus was randomized and ranged from 1000 - 6000ms, so that the stimulus was unpredictable. The six different stimuli were tested while standing and while walking, which meant each participant completed a total of 12 randomized trials (300 stimuli) for this study.

3.2.2 *Results*

Reaction time (RT) was calculated as the time between the start of the stimulus and the push of the button. 46ms of mechanical delay in the stimulus transducer was taken into account for the vibration modalities. Trials classified as mistakes included missing a response and pushing the button multiple times. The RT average only counted correct recorded pushes.

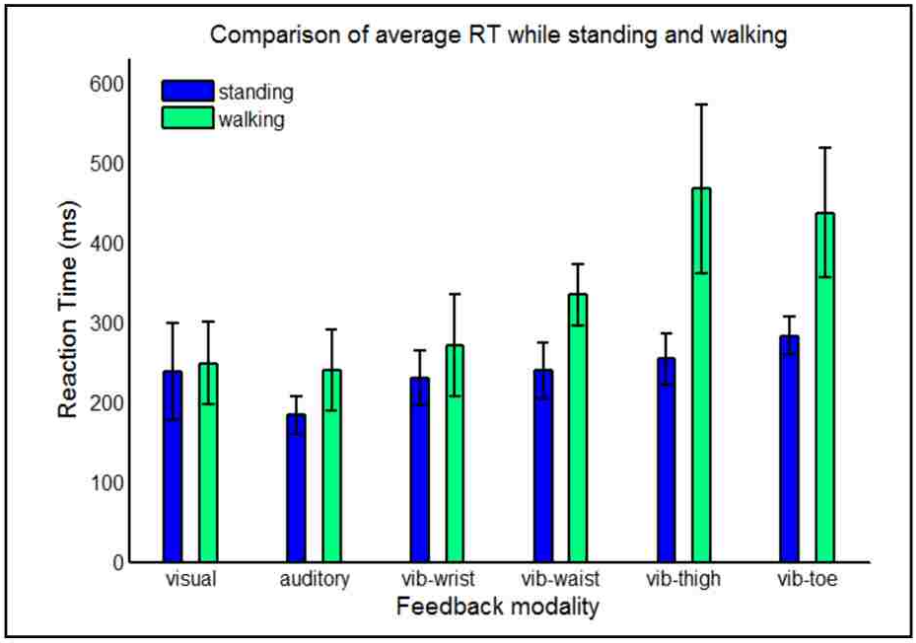

Figure 3.4 – Average reaction time for all modalities while standing and while walking.

Table 3.1 – Average reaction times (ms) and standard deviations.

Reaction Time (milliseconds)		
Modality	***Standing***	***Walking***
Visual	238.26±60.98	248.75±51.48
Auditory	183.69±23.68	240.13±50.54
Vibration-Wrist	230.33±33.89	270.85±64.53
Vibration-Waist	238.52±35.31	333.21±38.59
Vibration-Thigh	254.09±32.1	461.44±108.17
Vibration-Toe	283.3±24.14	437.2±81.01
All	238.03±32.62	331.93±96.88

Averages and standard deviations of RT for each modality were calculated and graphed in MATLAB. Figure 3.4 shows RT of each stimulus modality while standing and while walking. Specific average RT and standard deviations can be found in Table 3.1. The average RT of all modalities was 238.03ms while standing and 331.93ms while walking ($p=0.0482$). RT of auditory, vib-waist, vib-thigh, and vib-toe had significant differences between standing and walking ($p<0.05$).

To analyze the difference between modalities, a Joint Wald test was used instead of an ANOVA because a Wald test takes into account non-constant variances between subjects and modalities. Due to the vast differences in human reaction time, it is possible that some people have a very consistent response time while others may vary across a wide range. We tested the null hypothesis that the modalities all have the same mean RT against the alternative that they do not all have the same mean RT. Errors were noted for every individual's trials and averaged for each modality.

Using the Joint Wald test to compare each of the modalities while walking, Figure 3.5 shows thigh, toe, and waist vibration all have significantly higher RT than audio, which was the fastest RT. Table 3.2 shows that for walking, thigh vibration RT was 221.3ms slower than audio within subjects while the toe and waist were 197.06ms and 93.08ms slower than audio. In a separate Joint Wald test (Table 3.3), the differences (Walking – Standing) of each modality were compared. Both the thigh and the toe RTs were significantly affected by walking. Figure 3.5a shows the plot of walking RT for all subjects for all modalities and Figure 3.5b shows the RT differences.

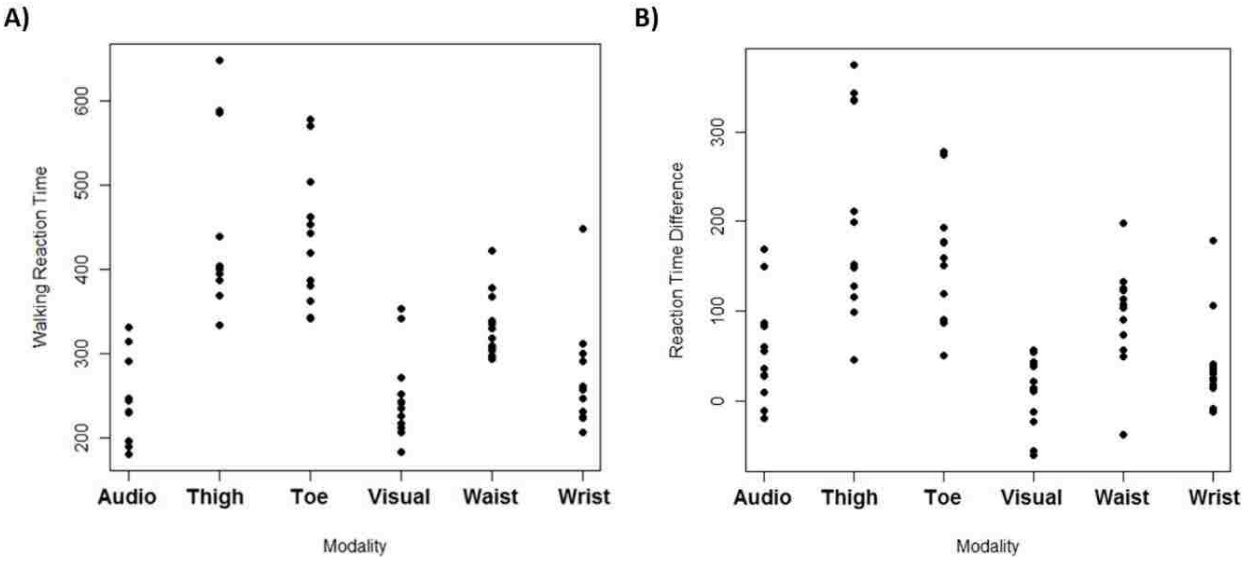

Figure 3.5 – A) Average walking reaction times for all subjects. B) Average reaction time differences (walking – standing) for all subjects.

Table 3.2 – Coefficients of different modalities for walking

Modality	**RT difference compared to auditory (ms)**	**p[a]**
Thigh	221.303	2.68e-13 *
Toe	197.063	1.26e-11 *
Visual	8.616	0.711054
Waist	93.080	.000177 *
Wrist	30.72	.189764

[a] Based on the Joint Wald test
* Joint Wald test: $p < 0.0001$

Table 3.3 – Coefficients of difference between walking and standing

Modality	**RT difference of walk vs stand compared to auditory (ms)**	**p[a]**
Thigh	150.903	22.92e-07 *
Toe	97.453	0.000399 *
Visual	-45.960	0.080832
Waist	38.247	0.144553
Wrist	-15.923	0.540297

[a] Based on the Joint Wald test
* Joint Wald test: $p < 0.0001$

Figure 3.6 shows the total number of errors made for each modality summed over all subjects and all tests. Toe vibration while walking resulted in the highest number of errors (13) while standing audio and standing wrist vibration both resulted in 0 errors.

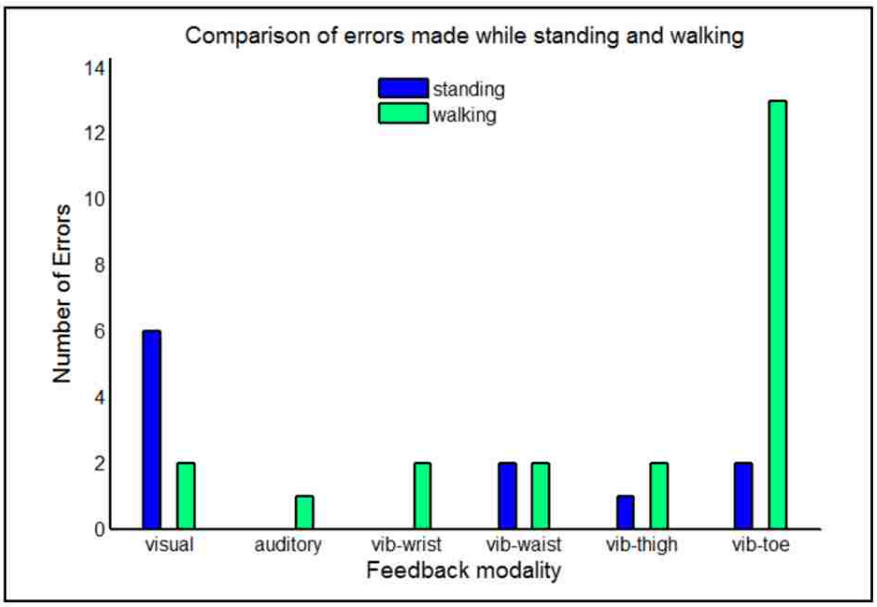

Figure 3.6 – Number of errors summed over all subjects and for all modalities.

3.2.3 *Discussion*

Based on the data, we see that auditory has the lowest average RT. The Joint Wald test tells us that we have strong evidence that different modalities do not all have the same mean. This is consistent with the plot in Figure 3.5 and the results in Table 3.3 suggest that the walking reaction time is higher than the standing reaction time, which we might expect. The differences are most pronounced in the thigh and toe. Unsurprisingly, the visual modality appears not to be very affected by standing/walking differences. The data supports our hypothesis that different stimulation modalities elicit different reaction times and that some modalities are more affected by walking than others.

Vibration at both the thigh and at the toe have the longest average RT, have higher rates of error, and are disproportionately affected when the user is walking. This could be a result of sensory overload, where a certain sense has reached its bandwidth and thus stimulating that sense is less noticeable [86], [88]. The lower limb undergoes more motion during walking, the muscles are extending and contracting, and the leg vibrates from impacting the floor. This could explain

why subjects informally reported after the experiment that they felt it was much more difficult to distinguish the vibrations on the toe and thigh than the other modalities.

Similarly, average occurrence of errors showed that most mistakes were made during the walking + toe vibration trial. 9 out of 12 participants erred during the walking + toe vibration trial while most of the other modalities elicited errors from only 1-2 people. It would be interesting to see where in the gait cycle the stimulus would cause people to err the most. This could affect whether stimuli should be given when muscles are contracted or relaxed or during a specific phase of toe off. However, the data collected from this experiment does not include gait cycle information.

The error data was intended to capture if a stimulus was missed or if subjects thought they felt a sensation that was not present. However, observation during the trials showed that many other factors affected each individual's error-rate. Some people would accidentally press multiple times or notice that they erred and miss the next press. These types of errors increase the error rate since one error can lead to two instances of error in the data.

The reason we included a toe vibration modality, even though lower limb amputees would not be able to utilize this feedback, is because most trip events occur at the toe. Figure 3.4 shows that response times were comparable between vibration at the toe and vibration at the thigh, thus validating that the thigh is a possible substitute for perturbation feedback. However, a true trip event may cause a reflex reaction that cannot be replicated by a simple vibration on the foot, which means the comparable RTs measured in this experiment may not hold true when a real trip occurs. Further research on how to trigger a trip-recovery reflex could be the key to designing a biomimetic feedback system.

In addition to trip warning, other types of feedback could also be useful to amputees that may not necessarily require a fast response time. The user of a prosthesis might want to know about socket fit throughout the day and be notified when socks need to be added or removed from the residual limb. Information about pressure distribution on the bottom of the foot could be useful when walking on stairs. Multiple motors could be used to give direction to help navigate through tricky situations.

If multiple motors are used, RT is also expected to increase due to Hick's Law [75], [89]. Hick's Law states that RT increases logarithmically with the number of choices a person has. Therefore, if a band of four motors were strapped around the thigh and subjects had to choose

which of the four motors were vibrating, we can expect the RT from this walking experiment to be much higher than 461ms. Similarly, if pairs of motors could also be actuated, then ten different combinations could be chosen from. We can see that RT will be significantly affected if multiple messages are to be sent through the feedback device. Further experiments to study the effect of a multi-motor system need to be performed in order to determine the optimal number of stimuli that can be used for a feedback device.

It is important to keep in mind that this data only represents RTs of healthy, young adults, which is theoretically the population with the fastest RTs [90]. Factors such as age and sensory deficits, which are often found in the amputee population, tend to increase RT [89]. However, certain trends in this data are likely to carry over to the amputee population such as slower RTs for sensory overloaded areas and more error for these modalities. Design of a feedback system for lower limb prostheses should take such factors into account.

RT is not the only factor to be taken into consideration during design of a feedback system. It is understandable that people may not want to be burdened with extra gadgets to wear and charge before they leave the house every day in addition to the prosthetic leg and liners that all amputees wear between their skin and the prosthesis. Devices that could be incorporated into the prosthesis/liners with acceptable cosmetics would be ideal. Considering ease of donning/doffing and cosmetics, vibrotactile motors embedded into the liner may be the best location for a feedback interface. Though our experiment did not test RT of vibrotactile motors embedded in a prosthetic liner, we believe these results should be similar to RT measured at the thigh. Because of slow RTs measured at this location, the type of information conveyed should not be RT dependent.

3.3 Differentiating Signals Around the Thigh

The purpose of this study was to measure reaction time and accuracy to multiple vibrotactile stimuli around the thigh while walking. Four Eccentric Rotating Masses (ERMs) around the thigh were actuated individually and in pairs, and subjects had to identify which motor(s) were vibrating while standing and while walking.

The device used in this experiment (Figure 3.7) included a band of four motors, hand-held buttons to submit responses, and the electronics component that vibrated the motors and recorded button presses and reaction time. The electronics contained an Arduino Mega 2560 microcontroller board that logged the test that was running, which button was pressed, and when the button was

pressed on a MicroSD card breakout board (Adafruit, New York). Subjects were asked to identify which motor(s) were vibrating by sequentially pressing the corresponding button(s) on a 3D printed clicker with four embedded tactile buttons. Vibrotactile feedback was given by an ERM motor (Precision Microdrives, London, UK) mounted in the suspension holder described in Chapter 2. The motors were evenly spaced around the thigh of the subject - anterior, posterior, medial, and lateral. Vibration of the motor could not be heard, so no additional actions were taken to mute the noise. Mechanical delay of the vibration motor on skin was tested by an IL-030 analog laser sensor (Keyence, Itasca) and measured with an oscilloscope (Tektronix TDS 30320). A 46ms lag was detected between ERM actuation signal and laser-measured skin displacement.

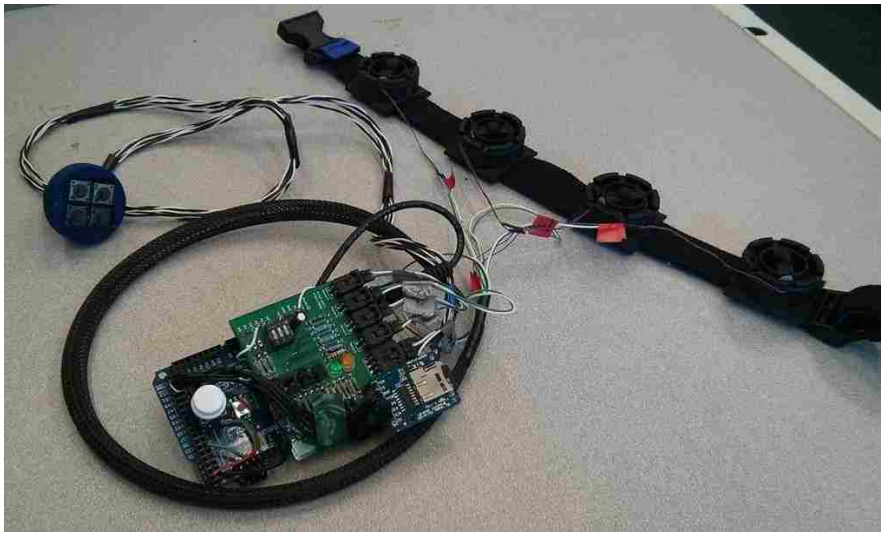

Figure 3.7 – Testing device: Response buttons (top left), four ERMs mounted in suspension holders on an elastic band (top right), and an electronics pack (middle).

3.3.1 *Method*

Subjects wore the band of four motors around the thigh of their dominant leg or in the case of amputees, the leg with the amputation (Figure 3.8). The response buttons were always held in the dominant hand and the electronics pack was either strapped around the waist or held in the non-dominant hand. In a randomly generated order, subjects performed three tests either while standing or while walking. In each test, all possible choices were presented five times with five nulls interspersed.

1) Single motor test: One motor vibrated (front, back, right, or left)

2) Double motor test: Two motors vibrated simultaneously (front back, front right, front left, back right, back left, or left right)
3) Mixed motor test: Either one or two motors vibrated (combination of above – 10 choices)

One healthy amputee (male, 40 years) and two non-amputees (2 male, average 24 years) were tested for these initial results. In addition to the three sets of standing and walking tests, subjects filled out a demographic survey and were tested by a licensed Prosthetist-Orthotist for signs of neuropathy. Tested subjects did not show any signs of neuropathy. The study was approved by the University of Washington Human Subjects Division (Study #44011).

Figure 3.8 – Subjects outfitted with the testing device.

3.3.2 *Results*

Reaction time (RT) was calculated as the time between the start of the stimulus and the push of the button. 46ms of mechanical delay in the stimulus transducer (ERM) was taken into account. Accurate responses required both button presses to be correct if two motors were vibrated. Note that the accuracy data was collected from 6 non-amputee subjects whereas the reaction time data only had 2 sets of data.

The average overall accuracy (all subjects and all tests) was about 83.28% and there does not seem to be significant differences between the amputee and non-amputees in terms of accuracy or reaction time (Table 3.4 and Figure 3.9). However, statistical differences were not calculated between the amputee and non-amputees due to the extremely low number of subjects.

Accuracy was significantly different ($p<0.05$) between the Single test and both Double and Mixed. This was true for standing tests and walking tests.

Figure 3.9 – Accuracy for each test condition.

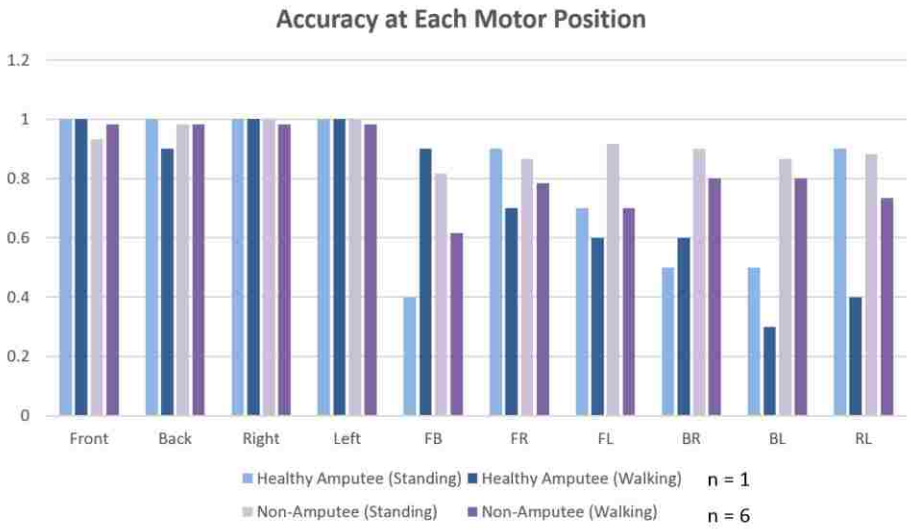

Figure 3.10 – Accuracy at each motor position for all tests. FB stands for Front and Back, FR stands for Front and Right, and so on.

Table 3.4 – Reaction time (seconds) averages for each test condition. For instances where two buttons were pressed, RT was recorded at each button press and 1st denotes RT of the first press and 2nd the second press.

Reaction Time (seconds)										
	Standing					**Walking**				
	Single	**Double**		**Mixed**		**Single**	**Double**		**Mixed**	
		1st	**2nd**	**1st**	**2nd**		**1st**	**2nd**	**1st**	**2nd**
Amputee (n=1)	1.10	2.24	3.08	1.19	1.84	1.49	2.2	2.62	1.85	2.47
Non-Amputee (n=2)	0.68	2.18	2.54	1.85	2.49	1.25	2.09	2.49	1.91	2.46

Table 3.5 – Comparison of the reaction time (seconds) between single motor and double motor instances during the Mixed Test. Only the 1st RT was considered in this instance.

Reaction Time (seconds) of Mixed Test				
	Standing		**Walking**	
	Single	**Double**	**Single**	**Double**
Amputee (n=1)	1.12	1.4	1.8	1.98
Non-Amputee (n=2)	1.6	2.11	1.9	1.89

3.3.3 *Discussion*

Both intact and amputee subjects did not have neuropathy or any lack of sensation at the tested site (lower-mid thigh), so results were not expected to show any significant differences. We can see that accuracy is highest for the single-motor test and that walking seems to have a small effect on accuracy. Subjects unofficially reported that the tests seemed significantly harder while they were walking. The data show similar trends for reaction time.

Because data was only collected from one healthy amputee subject, a statistical comparison was not drawn between amputees and non-amputees. However, we can see that the healthy amputee's response times and accuracies are comparable to healthy non-amputees that were tested. If this holds true of a larger healthy amputee population, then it would be possible to leverage

sensation/perception data collected from healthy non-amputees as an approximation for healthy amputee data.

The addition of multiple possible responses was expected to increase RT because Hick's Law states that there is a logarithmic increase in RT when subjects are faced with choices [75]. However, when subjects were faced with ten choices in the Mixed test, the RT of the first button press was faster than when only six choices were presented in the Double test. It is possible that response to single motors was much faster, and thus pulled down the RT average in the Mixed test. When we separate the Mixed test into single motors and double motors, we see that single motors had an RT of 1.36sec and double motors had an RT of 1.76sec while standing, and 1.85sec vs 1.94sec while walking (Table 3.5). Walking seems to generally increase RT and obscures the slight differences in RT when choice is involved. However, the results of this experiment are not conclusive and should be considered with care due to the extremely low n. More testing needs to be conducted to see if these results hold true.

3.4 CONCLUSION

These experiments provide a thorough comparison of human reaction time and accuracy in response to six different stimuli, performed while standing and while walking. The data collected can impact the development of devices for prosthetics, rehabilitation, haptics, etc. that may require knowledge of how quickly and accurately humans can respond to different stimuli. With the advent of new wearable technologies that are becoming trendy to wear (smart watches, smart glasses, stylish headphones), it is no longer a burden to wear an extra device. Instead of donning an extra vibration feedback system on the wrist, a system integrated into a smart watch that people might normally wear could provide a convenient from of feedback from a smart prosthesis.

Depending on the motivations that drive the design of a vibrotactile feedback device for lower limb prostheses, certain factors must be taken into consideration such as RT, error rates, location, and stimulus modality. If the design must relay information on a short time scale, vibrotactile stimulation on the leg may not be the ideal location for the actuator. Visual or auditory feedback would elicit the fastest reaction times. However, if the design must integrate an actuator into the liner on the thigh, the slow response time must be accounted for. Use of a proximity sensor could compensate for the slow reaction time and give users enough time to avoid tripping altogether. Other types of feedback could also be relayed to the user that does not depend on a fast reaction

time for action. Information such as socket fit throughout the day, whether to don or doff socks, directions, general information about the terrain, etc. are all possible types of feedback that amputees might be interested in knowing and could positively impact their ability to use their prostheses. To confirm the reaction time and accuracy of vibrotactile motors embedded in the liner and design prostheses with more relevant parameters, comparable data need to be collected on a larger sample size.

Chapter 4. LOCALIZATION OF TACTILE INFORMATION IN THE LOWER LIMB

Human ambulation requires a unique combination of motor control to direct the placement of the leg and sensory feedback to maintain balance. However, current lower limb prostheses only focus on the control aspect, which relegates amputees to navigate their environment through visual feedback and the limited sensory feedback that can be felt through the socket of the prosthesis. Poor balance on a prosthesis leads to decreased walking ability, increased risk of falling, and can even psychologically affect a person's willingness to walk due to fear of falling [12], [14].

The lack of sensory feedback for prostheses is slowly starting to be addressed through the advent of new sensory technologies such as microelectromechanical systems (MEMS) and development of better feedback techniques. MEMS provide increased sensitivity and better spatial resolution while still keeping the device small. Researchers have developed MEMS sensors for prosthetic/robotic hands and algorithms to explore shapes, edges, textures, etc. of a physical environment [91], [92].

One of the major missing components in making an effective sensory feedback system for lower limb prosthetics is how to transmit the haptic information back to the human user. This system requires multiple components that are heavily interdependent: 1) The device is usually subject to some size/resolution/weight/power constraint. 2) The location of delivery is usually determined by where such a device would be worn for a friendly user interface. 3) The dynamic situation to be conveyed through sensory feedback must be intuitive or easily learned. 4) Depending on the type of information, response time or accuracy or both may be important. All of these factors will affect the type of actuator that is used and its location on the body.

Researchers have studied the use of visual displays, speakers/headphones, vibrotactile motors, pneumatic balloons, and electrodes (electrotactile sensation) as feedback mechanisms for lower limb prostheses [33], [36], [37], [93], [94]. These sensory feedback modalities were applied to a variety of locations including the trigeminal nerve on the forehead, torso, and thigh [5], [25], [29], [31], [33], [34], [36], [37], [39], [95]. Most studies focus on providing feedback to the thigh because such a system could be used for both above knee and below knee amputees, and provide the most ideal user interface. This is why we have focused on the thigh and calf as sites where vibrotactile feedback could be integrated into a prosthesis.

In order to design a display system for the thigh/calf, we must understand the limits of perception on this area. Sensory feedback and spatial perception on the thigh or lower limb are not well studied compared to the hands. A few researchers have mapped spatial acuity using the two point discrimination test for the whole body, and the resolution of these studies were poor [96]. In previous work, at most one or two locations on the thigh, calf, and feet were tested [96]. Similarly, the work on spatial perception and memory of tactile feedback focuses on reading Braille or embossed letters with the hands [97], [98]. Only Wentink has looked at how location and stimulation affect perception of up to eight vibration motors on the thigh [38].

On the other end of the neural pathway, topographic mapping of the sensory system in the brain is limited to manual stimulations generated by the subject or delivered by experimenters. Many studies have drawn somatosensory homunculi using different imaging techniques of manual tactile stimulation. However, resolution of whole body mapping is often limited to only a few points on each region (usually up to 4 on the thigh, 4 on the calf, and maybe each toe) [99]. Increased resolution would require electrically driven systems, but common devices (vibration motors and mechanical actuators) interfere with typical brain mapping techniques such as functional magnetic resonance imaging (fMRI). Non-ferrous vibration devices have been designed, but the electronics that drive them still interfere with MR [100]–[105].Pneumatically driven devices are MR-compatible but only operate at lower frequencies (<150 Hz) [106], [99], [107]–[110]. An accurate and more detailed somatotopic mapping could deepen our understanding of the somatosensory system and allow us to more accurately assess plasticity after brain trauma or body injuries.

To improve our understanding of spatial perception of touch on the lower limb, I have developed a method to study spatial acuity and perception memory capabilities in a systematic way.

4.1 METHOD

12 non-disabled participants with an average age of 26 (SD 3 years, 4 male/8 female) were recruited for this study. All of the participants were recruited at the University of Washington and had no known sensorimotor deficits on the areas being studied. The study was approved by the University of Washington Human Subjects Division (Application #49225).

Washable markers were used to draw a grid of points on the thigh, calf, and foot. 10g disposable monofilaments (Medical Monofilament, Plymouth, MA) were used to provide pressure at each point (Figure 4.1). The monofilament provides a consistent 10g of pressure and will buckle to prevent the force from exceeding 10g. A computer program with graphical user interface was created in Qt (Version 5.4) for data collection (Figure 4.2). The window shows an image of the participant's leg area that is being tested, and the participant can mark on the screen where he/she felt was touched or submit "No Sensation" if no sensation was felt. MATLAB was used for data analysis.

Figure 4.1 – Experimental setup. Left: A paper grid is used to mark the grid on the thigh and subjects are seated in a position where they cannot see which points are being touched. Right: 10g monofilament that is used to touch each point until the monofilament buckles.

Three anchor points were marked on each area of the leg that was tested and a photo was taken at this time of each area. Coordinates of the anchor points were not chosen based on anatomical structures, just placed in an area where the entire grid would be visible on the camera. Grid lines were then drawn on each area. The thigh had a spacing of 2cm square and a total grid size of 5 x 6 points, the calf had 3cm square spacing and total grid of 3 x 4 points, and the foot had

a total of 20 points located based on foot features (distance between grid lines on the thigh and calf was determined from Nolan's paper [111]). Another photo was taken after the points were drawn that captures the anchor points and the grid.

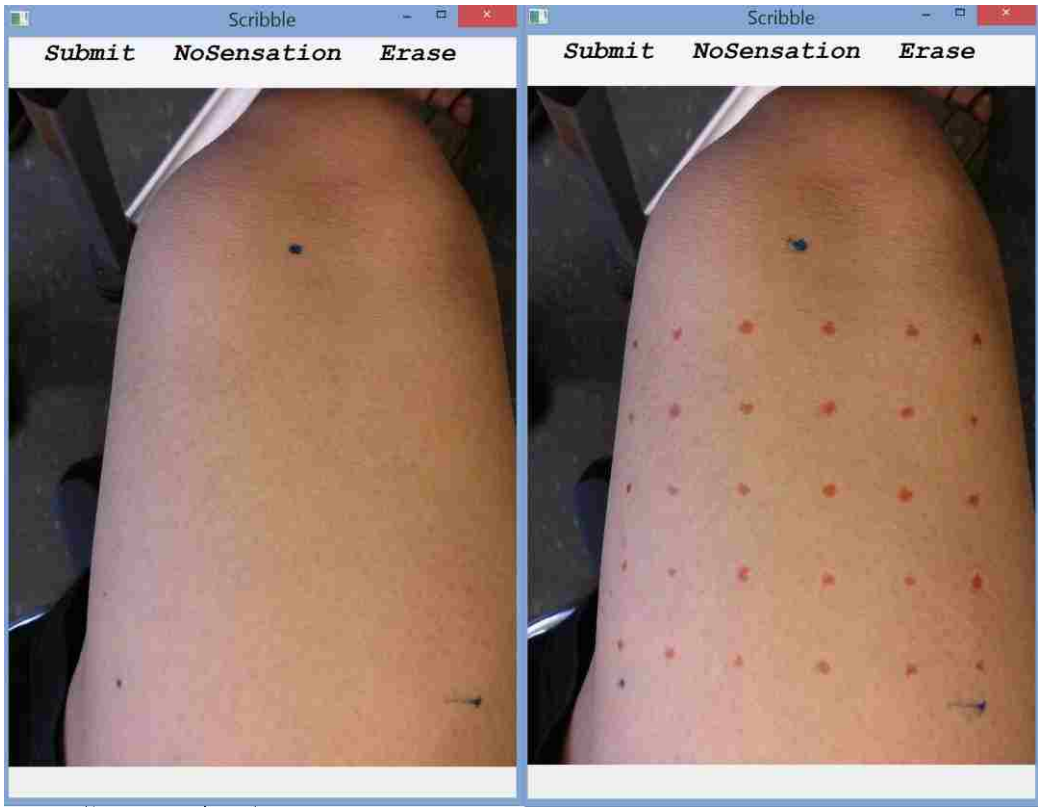

Figure 4.2 – Left: Example image shown during a No Grid test. Right: Example image shown during a Grid test. The three blue points are the anchor points and the red dots mark the points that will be touched with the monofilament.

Each subject's photos were loaded onto the Qt data collection program that presented the photos of each test location. A random sequence of points were generated for each subject that dictated the order in which grid points were touched by the experimenter with the monofilament fiber. The subjects were prevented from direct view of the contact sites by strategic placing of the laptop on which they recorded their answers. In the first experiment, subjects indicated touch locations on an image containing all grid points. Each grid point was touched a total of 5 times. They were asked to select with a mouse the point which was touched when they felt a sensation. In the second experiment, they were presented with the image of only the anchor points and no

grid points even though the researcher still touched points on the grid for an additional five touches each. Each grid point was touched a total of 10 times in this experiment.

All subjects were tested in the same order: Thigh with grid, thigh no grid, calf with grid, calf no grid, foot with grid, and foot no grid. At the beginning of each test, the three anchor points were touched to provide subjects with a reference.

4.1.1 *Data Analysis*

All pictures were taken with the same camera mounted on a tripod to ensure consistency between images of the same subject. The distance between the center grid points (C3 and C4 on the thigh, B2 and B3 on the calf) on each subject were measured to be 1cm on the screen of the camera to ensure consistency of image size between subjects.

In order to calculate the position of the true points of the No Grid experiments, images of the Grid and No Grid were aligned using the anchor points (Grid image was copied over the No Grid image and made transparent to line up anchor points - in almost all cases, only transposition was needed and not scaling) and merged in Photoshop. This image was then opened in the Qt software and each point was clicked in order to record the pixel location for comparison to subject responses. This last step was also performed for Grid experiments to record true pixel locations of each point.

In MATLAB, all subjects' data were normalized to Subject 1 by subtracting the difference between true grid points from all data.

```
[Subj1_truegridcoords] – [SubjN_truegridcoords] = [SubjN_normalizationvector]
     [SubjN_data] – [SubjN_normalizationvector] = [SubjN_normalizeddata]
```

The covariance matrix was calculated for each grid over all subjects and a 95% confidence interval of the error ellipse was calculated using the eigenvalues and eigenvectors of the covariance.

```
[eigenvec, eigenval] = eig(cov(data));
```

4.2 RESULTS

A single subject's data (Subject2) is shown for each of the locations and experiment types as a typical example of each subject's response.

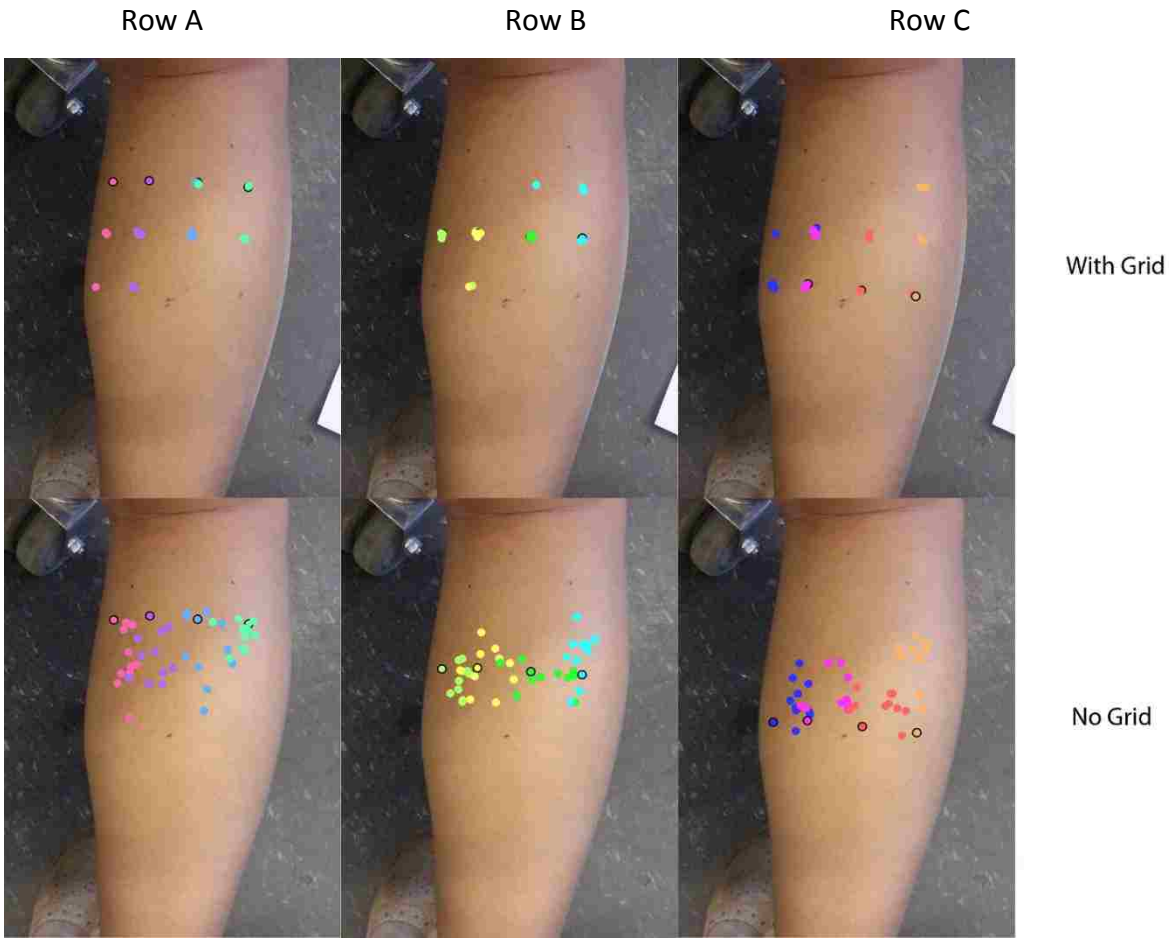

Figure 4.3 – Single subject calf data (Subject2). The images are separated into results from Grid and No Grid tests. The points are plotted by row (top to bottom) for clarity. The "true grid coordinates" are dots with a solid black outline and the responses of the subject at that point are plotted with the same color dots.

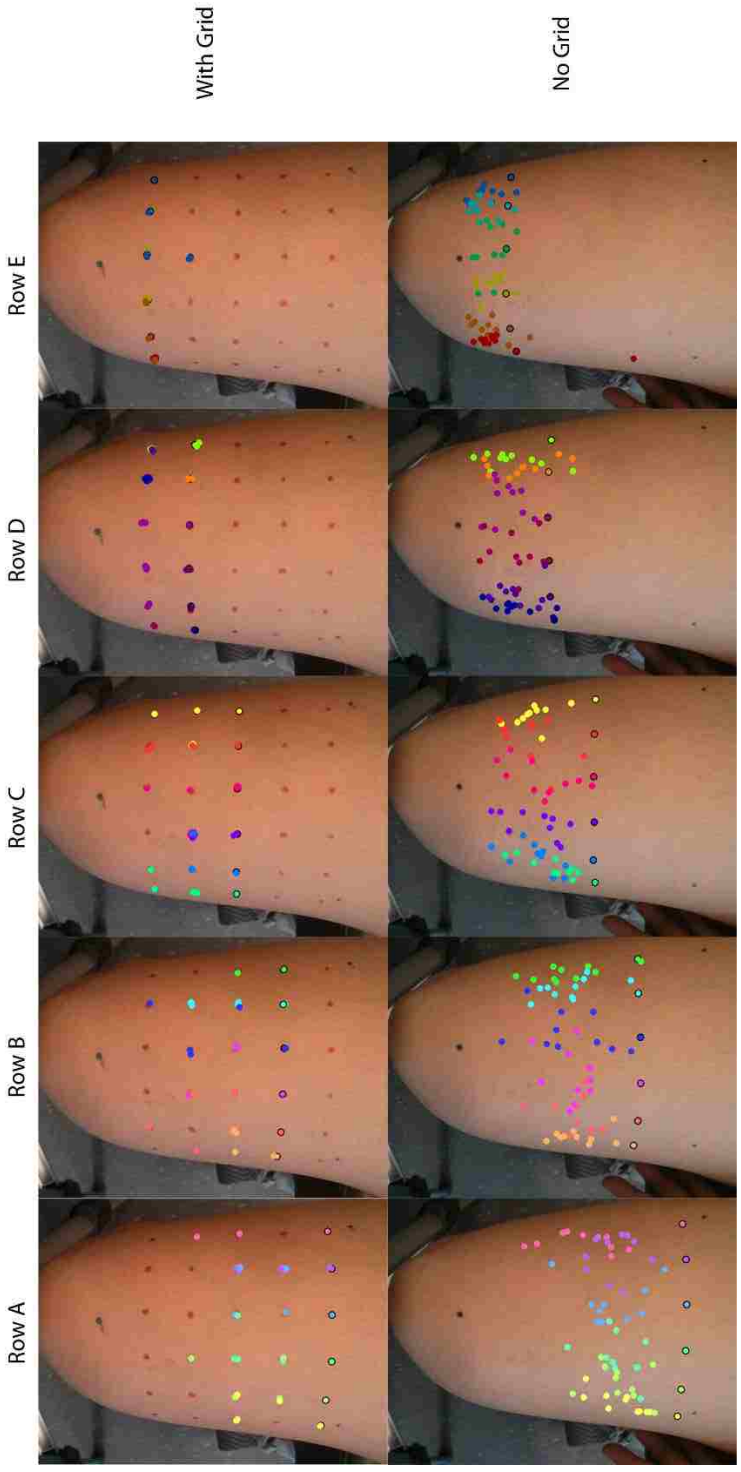

Figure 4.4 – Single subject thigh data (Subject2). The images are separated into results from Grid and No Grid tests. The points are plotted by row (top to bottom) for clarity. The "true grid coordinates" are dots with a solid black outline and the responses of the subject at that point are plotted with the same color dots.

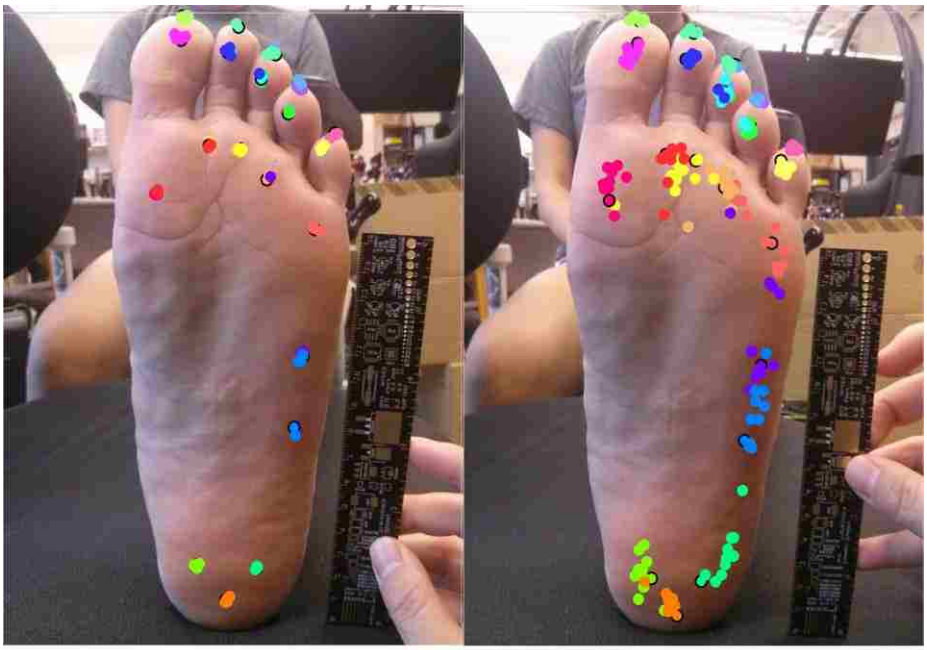

Figure 4.5 – Single subject foot data (Subject2). The "true grid coordinates" are dots with a solid black outline and the responses of the subject at that point are plotted with the same color dots.

Next, we present the combined normalized data for all subjects on the leg images of Subject1. Each set of points also includes a dotted ellipse that represents the 95% Confidence Interval, which means that 95% of the points fall inside of that ellipse.

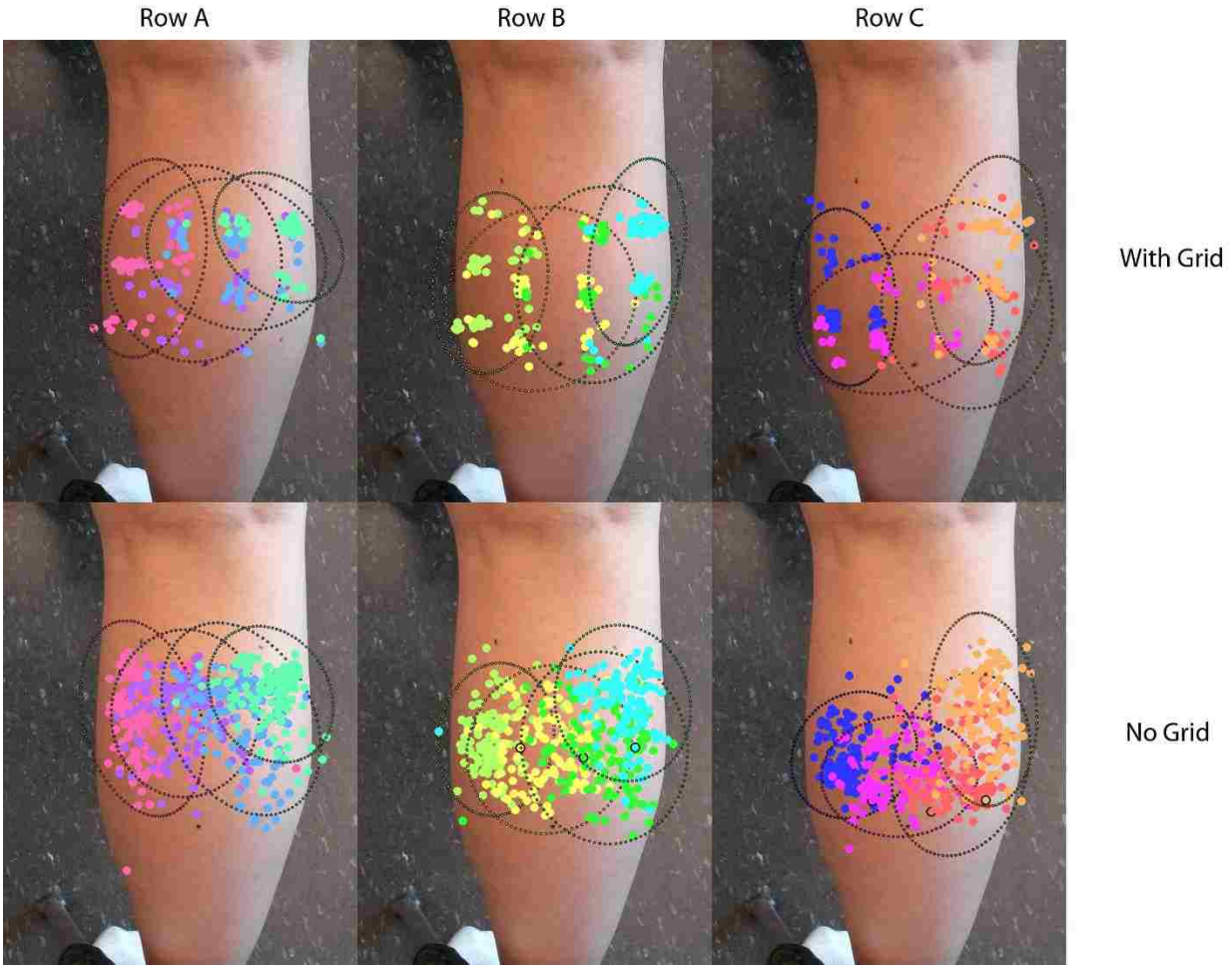

Figure 4.6 – Combined subjects' calf data normalized and plotted on images of Subject1's leg. The images are separated into results from Grid and No Grid tests. The points are plotted by row (top to bottom) for clarity. The "true grid coordinates" are dots with a solid black outline and the responses of the subjects at that point are plotted with the same color dots. The ellipses (of the same color as their corresponding data) encompass 95% of the points at their respective grid locations.

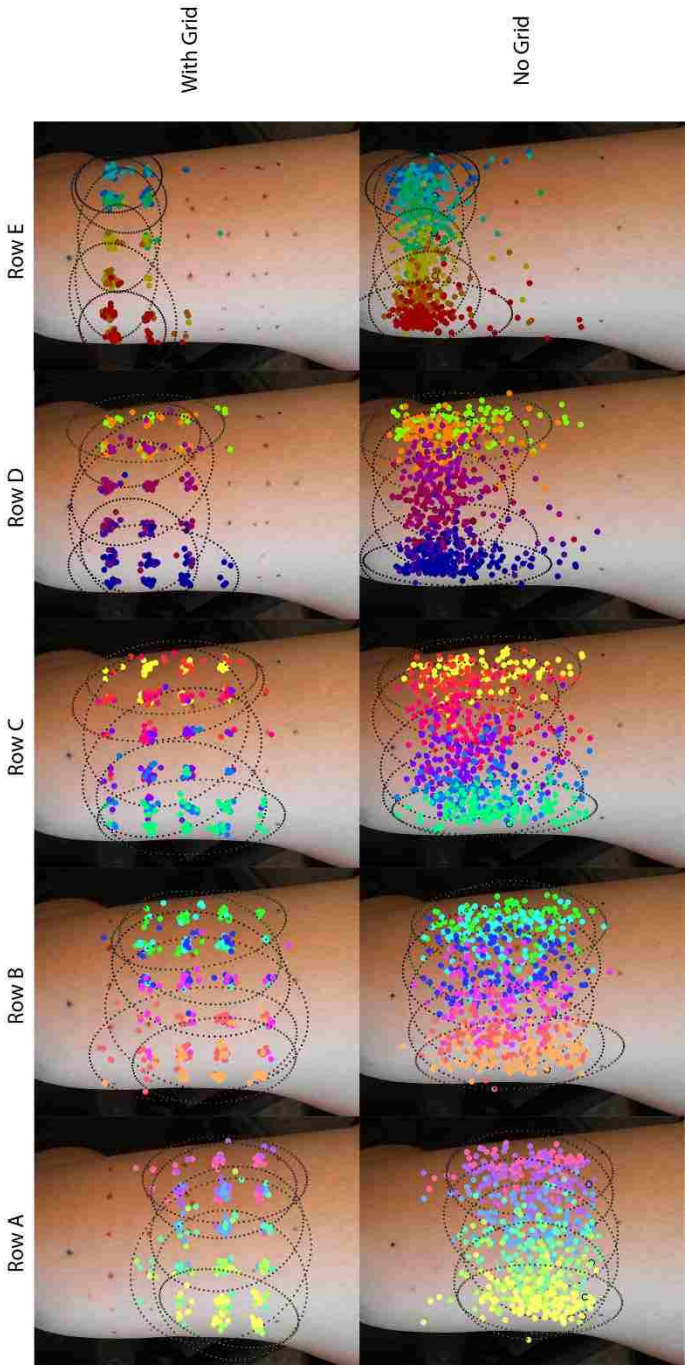

Figure 4.7 – Combined subjects' thigh data normalized and plotted on images of Subject1's leg. The images are separated into results from Grid and No Grid tests. The points are plotted by row (top to bottom) for clarity. The "true grid coordinates" are dots with a solid black outline and the responses of the subjects at that point are plotted with the same color dots. The ellipses (of the same color as their corresponding data) encompass 95% of the points at their respective grid locations.

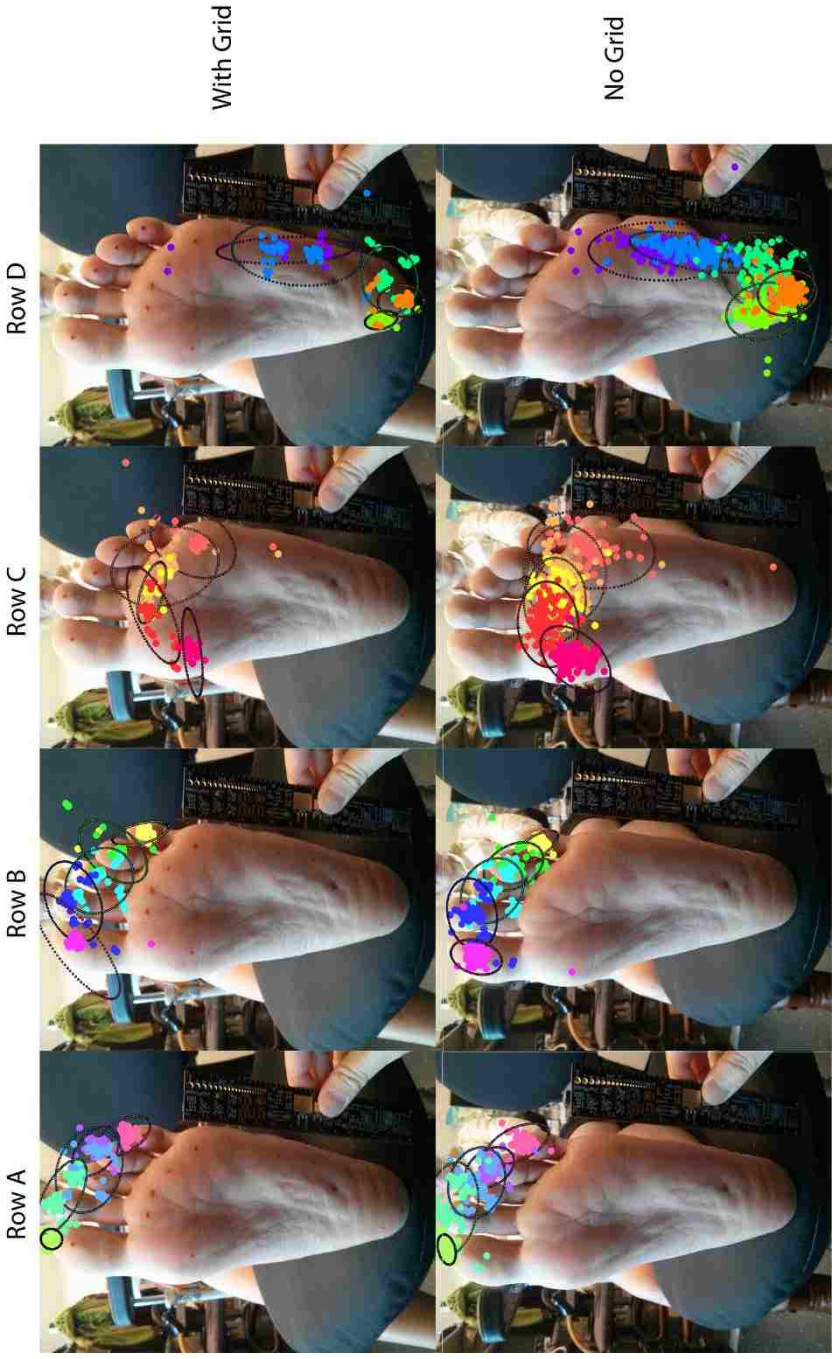

Figure 4.8 – Combined subjects' foot data normalized and plotted on images of Subject1's leg. The images are separated into results from Grid and No Grid tests. The points are plotted by row (top to bottom) for clarity. The "true grid coordinates" are dots with a solid black outline and the responses of the subjects at that point are plotted with the same color dots. The ellipses (of the same color as their corresponding data) encompass 95% of the points at their respective grid locations.

Accuracy – Calf (Grid)

16.7%	30%	33.3%	43.3%	30.8%
28.3%	28.3%	36.7%	25%	29.6%
38.3%	21.7%	13.3%	6.67%	20%
27.8%	26.7%	27.8%	25%	

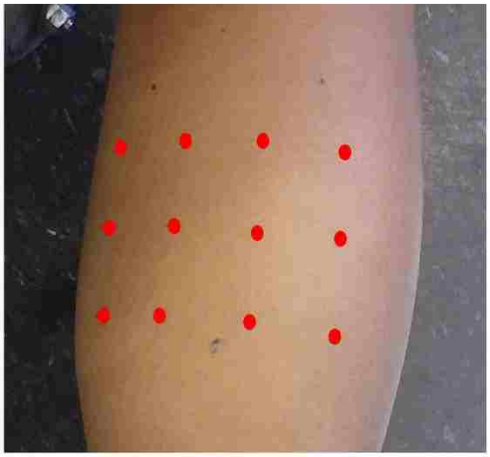

Accuracy – Thigh (Grid)

50%	30%	33.3%	30%	51. 7%	40%	39.17%
21.7%	28.3%	18.3%	28.3%	31.7%	28.3%	26.1%
20%	18. 3%	13%	13%	13%	13%	15.28%
10%	6.7%	15%	15%	20%	13.3%	13.3%
26.7%	6.7%	6.7%	20%	15%	18.3%	15.56%
25.67%	18%	17.33%	21.33%	26.33%	22.67%	

Accuracy – Foot (Grid)

100%	61.7%	45%	78.3%	78.3%	72.7%
95%	70%	58.3%	80%	93.3%	79.3%
98.3%	61.7%	63.3%	65%	81. 7%	74%
				76.7%	75.7%
				46.7%	
	98.3%		66.7%		
		90%			
95.8%	72.9%	58.3%	67.5%	82.5%	

Figure 4.9 – Average accuracies at each point. Blue cells denote averages of the row/col.

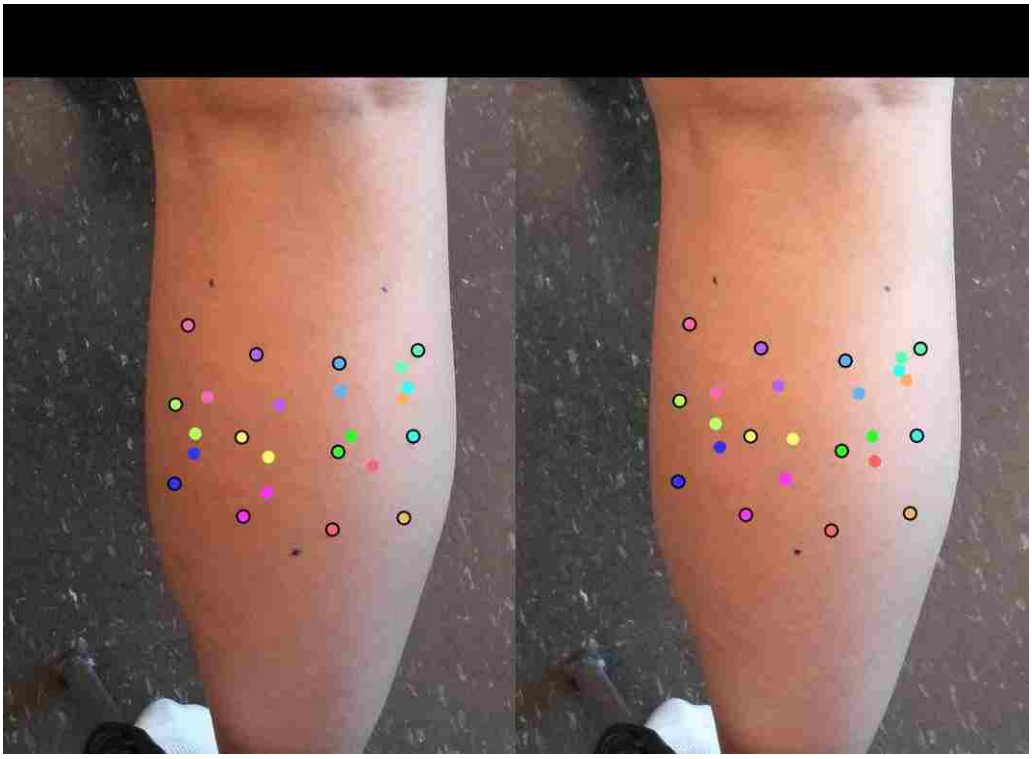

Figure 4.10 – Centroid of ellipses on calf (corresponding color) in relation to actual touched points (black outline).

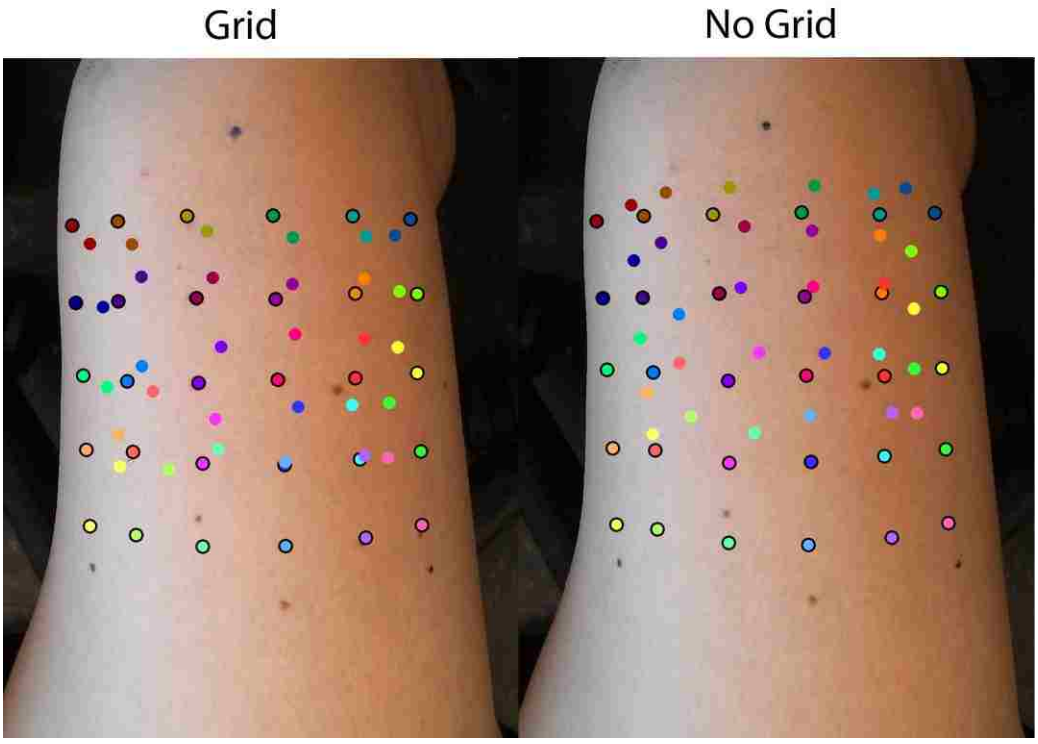

Figure 4.11 – Centroid of ellipses on thigh (corresponding color) in relation to actual touched points (black outline).

Figure 4.12 – Centroid of ellipses on foot (corresponding color) in relation to actual touched points (black outline).

4.3 DISCUSSION

Figure 4.9 shows that spatial distinction of medial/lateral sensations (columns) are on average more accurate than in the proximal/distal (rows) direction for the thigh. Columns of the thigh were accurate at a rate slightly higher than chance whereas the rows were typically below chance except for the last two (most distal) rows. The calf accuracies were the least accurate since they were very close to chance in both the row and column comparisons. Data collected on the foot shows extremely high accuracies for columns 1 and 5, which are in large part due to peoples' abilities to distinguish the big toe/ball of foot and the pinky toe/outside of foot. Points in the middle of the foot (medial-laterally, toes 2-4) tended to be confused with each other and could not be spatially identified as well as the big toe or pinky toe sides. Based on the design of the study, grid sizes were chosen relative to each area's two-point discrimination threshold. This should have resulted in similar accuracies across the three locations, but average subject performance trended with the spatial acuity of each area. The ability of people to spatially locate a point that was felt was strongest on the foot, then the thigh, and the calf was the least accurate.

Figures Figure 4.3 andFigure 4.8 show that responses corresponding to the actual point create noticeable columns in the medial/lateral direction, while these columns tend to span the entirety of the proximal/distal distance. The one exception seems to be the most distal row of points on the thigh. This row has the smallest error ellipses and the highest percent accuracy compared to any of the other rows on the thigh (Figure 4.9). People may not have been able to spatially distinguish how proximal/distal the center rows were, but the most distal row was not often mistaken to be proximal. One explanation of this result is that mechanoreceptor density on the lower limb tends to vary more from proximal to distal than medial to lateral. It is also possible that our memory of perception is better in the mediolateral direction because there are more spatial cues/reference points to aid our visual cortex in developing a mental image of the thigh [112].

The dermatome maps which areas of the body are supplied by which spinal nerves. On the lower limb, the dermatomes are vertically separated to divide the leg into columns Figure 4.13. This could also explain the ability of subjects to differentiate between columns than rows. Points in different columns may map along different dermatomes while points in the same column are more easily confused because they are within the same dermatome. It would be interesting to see how this data maps onto the dermatome and whether this hypothesis is correct. If so, this could mean that other areas of the body may have similar spatial perception trends that align with the dermatome. No research has been performed on whole-body sensory capabilities at such high resolution, so this information would be very valuable to infer properties of sensation for less studied areas.

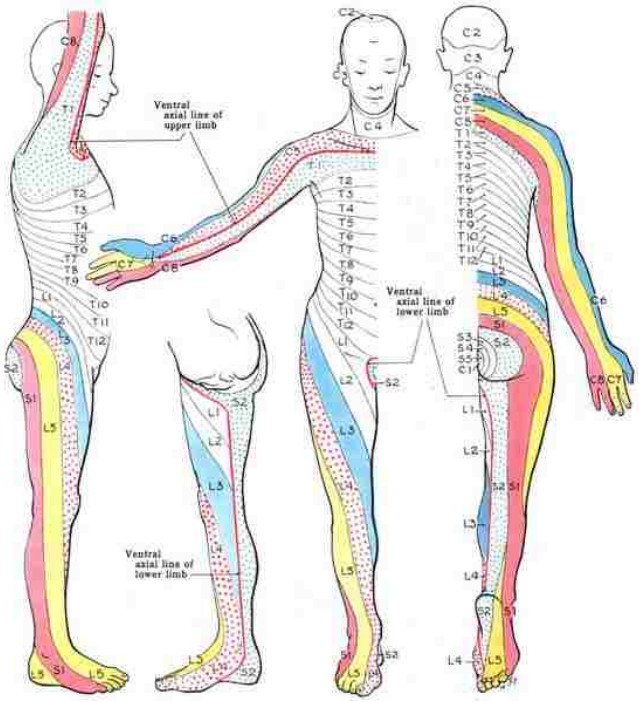

Figure 4.13 – Map of human dermatome [113]

The error ellipses for both Grid and No Grid experiments were similar, which means that selecting a point from a grid versus marking a point on a picture had little effect on the spatial memory of perception. We originally hypothesized that gridded and non-gridded tests would generate different results due to a bias when people are shown a grid and told one of these is the "correct answer" whereas the No Grid experiment truly captured where subjects perceived the sensation. The centroid of the ellipses (Figure 4.10, Figure 4.11, Figure 4.12) can be differentiated between each other and create a grid only slightly offset from the actual grid points. This means a bias existed that rather uniformly shifted perception (memory of perception) in a certain direction.

Something to note is that subjects were consistently able to distinguish where a point was relative to the last point touched. The location of the actual sensation may be reported in the wrong place, but the direction relative to the last point was usually correct. This shows that a person's ability to spatially remember perception is rather short. They can compare the currently felt point to the last felt point, but cannot spatially remember enough points (such as the reference points) to exactly locate where the current touch is.

Error in the system could be due to the 2D response interface to a touch on a 3D surface. The curvature of the leg will cause the image of the grid to vary in pixels in the medial/lateral direction.

This could be corrected for by using a 3D image in the response interface or by compensating for the curvature when processing the data. However, the poor spatial resolution of perception on the leg (on the order of 2-3 centimeters) may not be largely affected by the few millimeters that this error would account for.

Based on our findings, two rows of motors could be used on the thigh if they were separated by about 8 cm, and at least a 5 cm spacing would be needed for motors placed mediolaterally. The calf should only have 1 row of motors and multiple motors should be separated by at least about 9 cm. It would be important for sensors on the foot to capture sensory data on the medial and lateral sides, but fewer sensors are necessary for the middle since it is clear that people have trouble distinguishing between toes 2-4.

In this chapter, we have developed a method to systematically analyze spatial acuity and showed results of this analysis on three areas of the lower limb. Additionally, this spatial acuity analysis method could be used to study the mechanisms of reinnervation and/or cortical remapping after Targeted Muscle Reinnervation (TMR) surgery, which will be expanded upon in the next chapter.

Chapter 5. LEVERAGING NATURAL SENSORY FEEDBACK

5.1 NERVE REGENERATION

In the peripheral nervous system, nerves can regenerate depending on the level of damage sustained. When a peripheral axon is crushed or severed, there will be some macrophages to phagocytose the dead tissue, but also an influx of Schwann cells that are the main factor in axonogenesis. In some cases when the sheath is still intact, nerves can reconnect with their original target. However, if the tubes are disrupted, it is possible for regenerating sprouts to enter inappropriate distal stumps [114]. One theory behind restoration of original innervation patterns is that specificity can originate when target muscles/areas release cues for neuronal growth. Alternatively, Schwann cells and fibroblasts could provide cues for growing axons [115]–[117]. Regenerated nerve fibers can sometimes have slower response times and higher action potential thresholds than normal axons due to shorter distances between gaps in myelination and possible formation of scar tissue [114]. One of the likely outcomes of amputation is that severed nerves can undergo unregulated regeneration and become painful neuromas. Depending on the severity of the neuroma, more surgery may be needed to remove the growth. One of the surgical techniques being studied to prevent neuroma growth is targeted muscle reinnervation.

5.2 TARGETED MUSCLE REINNERVATION

Targeted muscle reinnervation (TMR) is a surgical method that was originally developed by Dr. Todd Kuiken and Dr. Gregory Dumanian at Northwestern University [118]. This technique transfers the nerve that formerly controlled the amputated limb to a muscle that would otherwise be rendered useless due to the amputation [118], [119]. In the most common examples of TMR (Figure 5.1), the nerves that directed hand function were reinnervated to either the upper arm or the chest region depending on the level of amputation [120]. The same technique can also be applied to lower-limb amputations where the nerve controlling the foot could be reinnervated at the calf or on the thigh depending on the level of amputation [121]–[123]. The location where the nerves are reinnervated is called the TMR site.

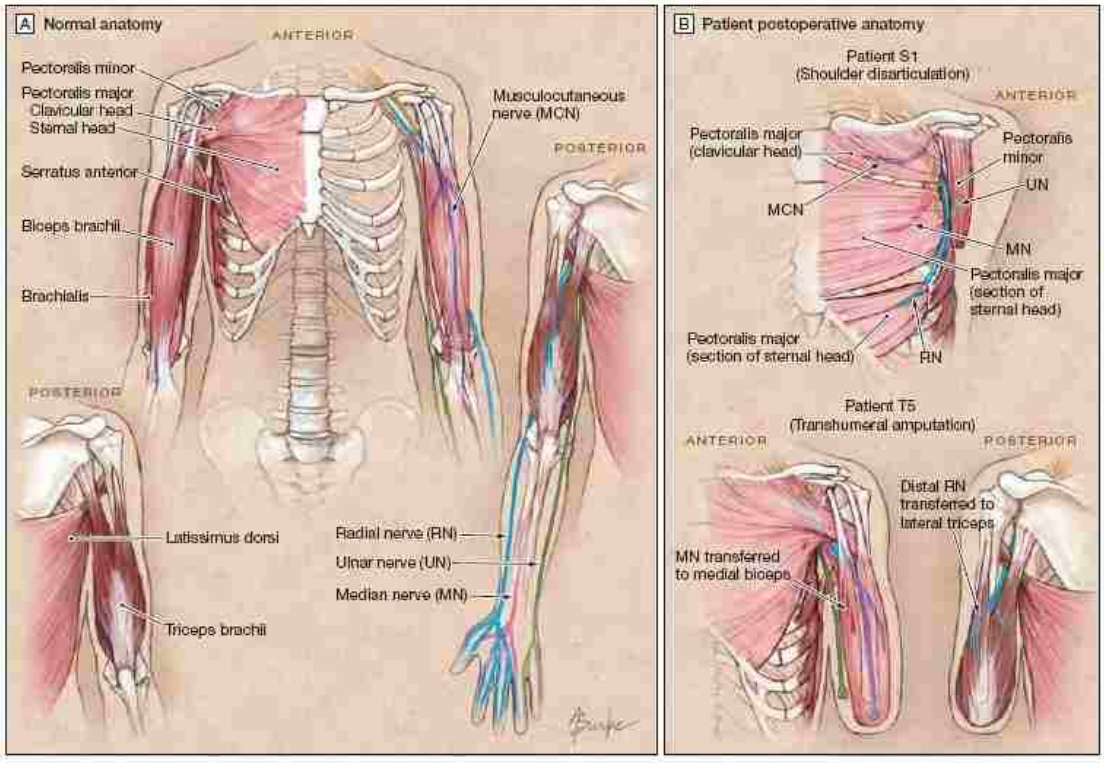

Figure 5.1 – Diagram of where nerves are relocated in upper-limb TMR surgery [120].

When reinnervating nerves into a new environment, it is difficult to predict how they will grow. It is thought that nerves will probably seek to reinnervate similar structures such as muscles or mechanoreceptors [114]. The physiology of this phenomenon is not well understood, and possibly related to experiences of phantom limb sensation [16], [17], [124]–[127]. The reported results of TMR are equally unique and can best be described as a "controllable" phantom limb sensation. When patients "thought" to move their hand, signals would be sent from the brain to the nerves that originally controlled the hand. However, these nerves now innervated the chest/upper-arm muscles and caused them to fire, which can be read using an electromyography (EMG) sensor [118]. Conversely, when the TMR site was touched, patients reported that they felt their phantom limb was being touched [21], [22]. In multiple patient case studies, both efferent and afferent communication with the missing limb can be accessed through the TMR site [21], [22], [118].

5.2.1 *TMR Used for Myoelectric Control of Prostheses*

The first application of the effects of TMR was to utilize the efferent signals and control upper-limb myoelectric prostheses. Myoelectric prostheses use EMG signals (electrical signals

generated when muscles contract) to control motorized arm joints [118], [120]. Current myoelectric prostheses use only 1-2 EMG signals that can be found on the residual limb, and depending on the number of joints available to control, may require users to manually switch between different modes and actuate joints one by one. This method is slow and unintuitive, making it difficult to learn and hard to operate [121].

The advantage of TMR is that physiologically appropriate EMG signals can be sent by the user to control multiple joints on a myoelectric prosthesis. Patients who have undergone upper-limb TMR surgery have been able to intuitively and simultaneously control multiple joints including opening and closing of the hand and extension and flexion of the elbow [128], [129].

Functional tests for upper-limb TMR subjects were reported by Miller in a 2008 Case Study [130]. Patients who had undergone TMR surgery, recovered, and been fitted with a myoelectrically controlled prosthetic arm were asked to perform two timed tasks - the Box and Blocks test and Clothespin Relocation Task. This experiment compared their ability to perform the tasks pre-TMR and post-TMR using the same prosthetic arm, and in all cases, post-TMR tests showed marked improvement. EMG control after TMR had been reported to increase speed of task performance by 2- to 6-fold and patients self-reported an increase in ease of function and use [130]. In a separate study, Miller showed one subject's ability to control a 6 degree of freedom arm in multiple tasks (Figure 5.2 left) [128]. Some of these tasks required controlling multiple functions simultaneously and could not be performed pre-TMR [128].

Figure 5.2 – Left: Subject performing the Clothespin Relocation task [128]. Right: subject fitted with an array of EMG sensors to map muscle activity following TMR [129].

Lower-limb prostheses are traditionally not EMG controlled - the ankle joint is typically passive and the knee may have a microcontroller that requires manual mode selection. Using EMG to control a lower-limb prosthesis adds an extra layer of complexity because walking/sitting/walking on hills/etc. may accidentally trigger an EMG signal to change modes unexpectedly [6], [123]. With the help of pattern recognition techniques, Hargrove has shown that it is possible to accurately classify motion intent in a virtual environment using EMG signals from the leg [123]. In a more recent study, TMR on the lower-limb has been shown to improve real-time classification accuracies and resulted in much faster movement of a virtual limb [121]. As classification and control algorithms improve, it is likely that myoelectric lower-limb prostheses for TMR patients and non-TMR patients will be seen in the future.

5.2.2 *TMR and Sensory Feedback*

The properties of sensory feedback at TMR sites were further studied by Kuiken's team. They performed rigorous studies on cutaneous sensation of the reinnervated areas by characterizing touch sensation, temperature thresholds, and electrical stimulation of 2 TMR patients [21], [22]. An area of 15cm wide by 17cm high on the chest was mapped to phantom upper-limb sensations (Figure 5.3). Within this area, the center would elicit only missing limb sensations whereas the edges tended to elicit both missing limb and chest sensations. It is likely that dual sensations may be due to regeneration of native chest nerves at the site of TMR. These studies show that robust sensations can be projected onto the missing limb after TMR.

Schultz looked at vibrotactile detection thresholds on the TMR site compared to the contralateral side (for the unilateral amputees) and found that vibration-detection ability was preserved, suggesting successful functional reinnervation of the mechanoreceptors [131]. Though vibrations applied to the TMR site were perceived on the missing hand, the detection threshold data (vibration frequency and amplitude) were more reflective of chest or arm thresholds than hand thresholds. This result suggests that the environment into which the afferent nerves of the missing limb were transferred has a large influence on sensation characteristics after TMR [131].

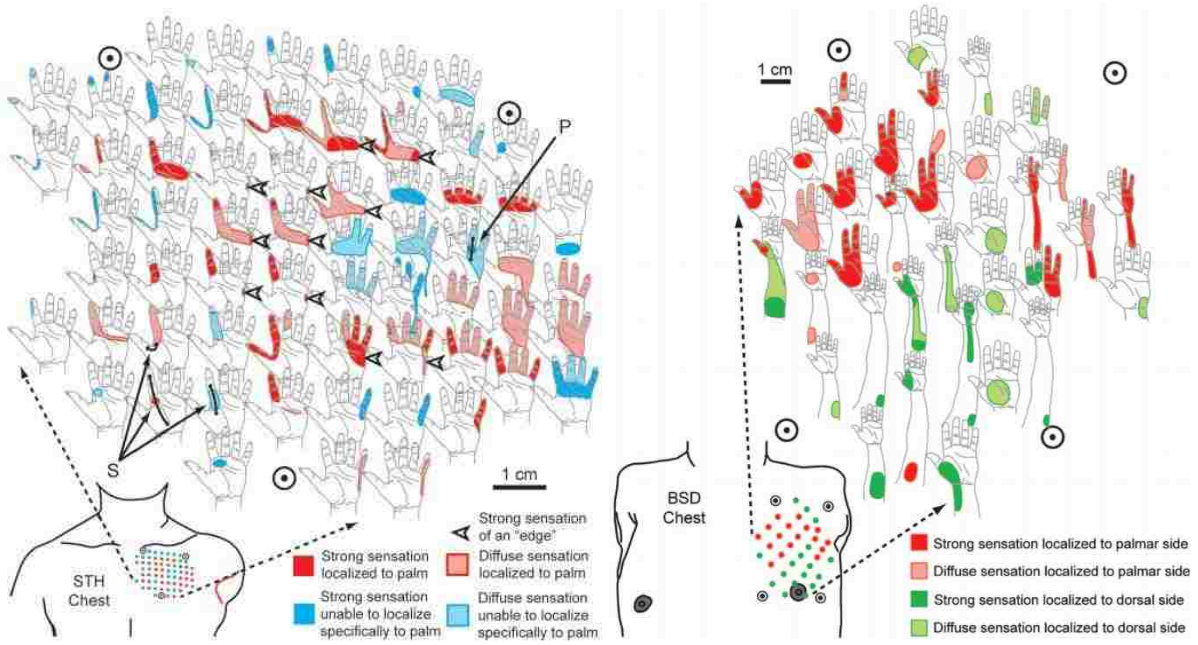

Figure 5.3 – Phantom limb sensations mapped to TMR sites on two different patients [22].

Marasco further studied the sensory capacity of the reinnervated area using a grating orientation task and point localization task. Grating orientation abilities correspond to sensory receptor innervation density while point localization involves cortical interpretation [21]. His research focused on whether recovery of sensory feedback is more influenced by receptor density or by the cortical area devoted to the skin surface. Due to the disparity between the hand and chest in receptor densities and the area of the brain that processes the sensory information, it becomes an interesting question what will happen after reinnervation. Marasco found that the grating orientation at the normal chest and the reinnervated chest were similar, but touch localization ability at the reinnervated region was increased. These results show that relative acuity of peripheral receptors may be related to the amount of central processing area devoted to the inputs [21]–[23].

5.3 Developing Natural Sensory Feedback for Lower Limb Prostheses

Much of the original TMR work was performed on upper-limb amputees [21]–[23], [118]–[120], [128]–[132]. Work on lower-limb TMR patients thus far has mainly focused on efferent signals to control EMG prostheses [121]–[123], [133]. Therefore, gaining a better understanding

of sensory reinnervation after TMR in lower extremity amputees may enable novel prosthetic legs with real-time, intuitive, sensory feedback of sensed quantities in the foot relevant to balance and robust walking.

In lower extremity TMR patients, real-time intuitive sensory feedback of information, such as the center of pressure on the sole, or contact with the front of the toe, if fast enough and intuitive enough, could prevent falls. In other words, TMR patients could have sensory feedback localized to areas of the missing leg that standard amputees do not possess. This opens the door to new technologies that utilize and maximize the sensory capabilities introduced by TMR.

Current research on trip warning devices depends on the user's ability to learn and respond quickly to a new signal [35], [36], [134]. In contrast, using TMR would provide amputees with sensations that already map to pre-amputation sensorimotor locations in the body and brain, decreasing the response latency relative to a learned, unnatural reaction. Thus the goal is to allow amputees to feel the prosthetic leg as if it were his or her own. If connected to appropriate information with sufficiently low latency, this new information may help prevent falls, while also decreasing rehabilitation time and increasing an amputee's "sense of self" when wearing a prosthesis [23], [135]. Instead of seeing the prosthetic device as a tool, amputees may feel that the prosthesis is part of their own bodies and develop more intact self-images [23], [136]–[138].

Based on the identified benefits that TMR has to offer, the next step is the development and validation of the ability to provide natural sensory feedback to a TMR site (Figure 5.4). This would lay the groundwork for a myriad of future studies including embodiment of a prosthesis, sensory rehabilitation techniques, and field studies (functional system validation) to see if sensory feedback improves a person's ability to use a prosthesis. If successful, this study has the potential to change the entire prosthetics industry.

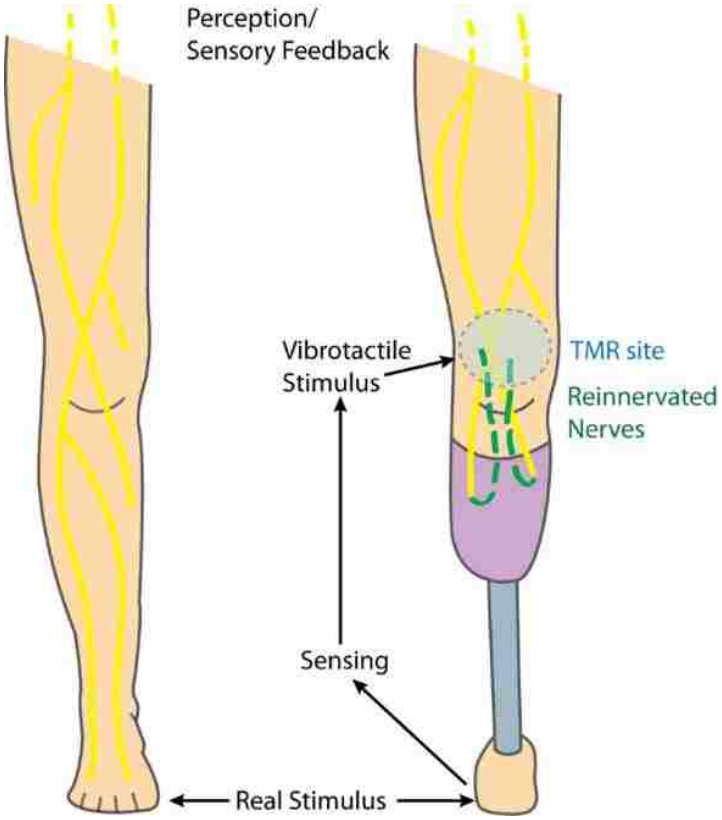

Figure 5.4 – Diagram of a potential system that utilizes TMR effects to provide natural sensory feedback.

Chapter 6. CONCLUSION

Having developed an optimized vibrotactile display for the leg, we found that this system elicited the fastest response time when worn on the wrist (270ms) compared to the lower limb (461ms on thigh and 437ms on toe) when subjects were walking. Auditory feedback was found to elicit the fastest reaction time while walking of all the modalities (240ms). Based on these results, the use of a sensory substitution system may not be feasible unless movements are predicted or time-sensitive information is not being communicated.

It would also be prudent to look into other types of information that amputees would want fed back while using their prosthesis that does not depend on fast reaction time. Additional data collection both on amputees and non-amputees is required to calculate statistics more representative of the population. However, it could be said that since data was collected on the population with the fastest RT, a system that is too slow for this population would also be too slow for the target population.

Slow RT could be due to a variety of factors - learning curve due to non-intuitive feedback (sensory substitution), too much stimulation in the lower limb due to walking (sensory overload), and the introduction of multiple choices (using four motors around the thigh).

One opportunity of stepping away from this sensory substitution feedback system is to leverage the natural sensory feedback capabilities after TMR surgery. It is possible that this method is more intuitive and can take advantage of natural reflexes triggered during a trip response, no longer depending on RT of a learned reaction. Not only would a prosthesis be safer to use, but the embodiment of the prosthetic limb could lead to better self-image and decreased phantom limb pain. The advent of technologies leveraging the benefits of TMR surgery could change the entire landscape of prosthetic devices.

6.1 FUTURE WORK

6.1.1 *Robotic Mapping of Sensation at TMR Site*

Although sensory reinnervation has been reported in the upper limb using manual methods, testing sensory responses by manual means is well known to be subject to potential biases such as the “Clever Hans” effect (in which unconscious experimenter reactions trigger behavior changes).

Valid mapping of TMR sensory responses and locations will ultimately require objective double-blinded methods. Repeatable and unpredictable tactile stimuli can be provided to the TMR site using an existing, intrinsically safe, robot, the Raven-II™ [139]. Patient responses will be objectively collected using a computer application in which they will click the location or outline the region of perceived stimulation (or click an icon to indicate no perception) similar to the interface used in Chapter 4.

We propose to exploit available robotic and computer technology to design a mapping process in which the location and nature of the test contacts will not be known to either the patient or the researcher to ensure that our results are not biased. This will eliminate researcher and patient bias from the mapping step and set the stage for the most rigorous validation test of sensory TMR maps.

Figure 6.1 – Representation of proposed TMR mapping setup. A pre-defined grid of points (on the location to be tested) will be gently touched by the Raven-II robot (right). A Microsoft Kinect sensor (bottom left) will map the 3D surface in real-time and help guide the robot.

The first steps of implementing a robotic mapping technique are already under way. Sharon Newman is developing Raven code (Figure 6.2) that will use a Microsoft Kinect to track where grid points are drawn on the leg, then command the robot to touch each point using a monofilament or vibrotactile device (Figure 6.1). The software to collect user response will be similar to the one described in Chapter 4, but provide a 3D rendering of the leg instead of just a 2D image.

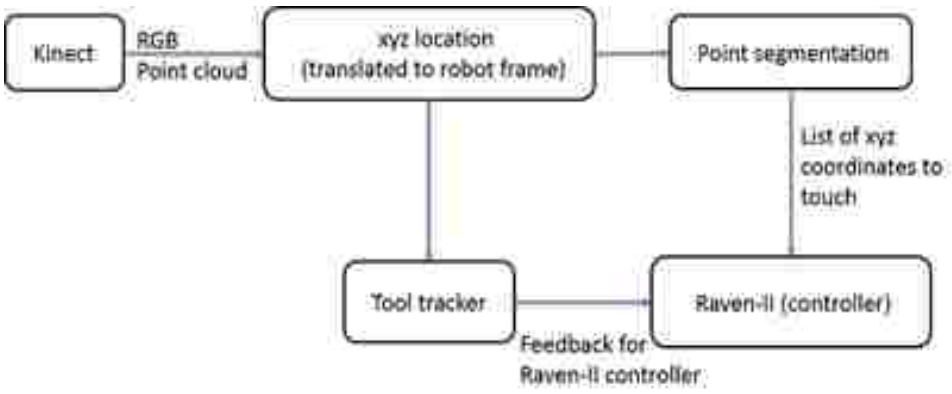

Figure 6.2 – Diagram of ROS nodes for Raven-II control to generate gentle touches at the marked locations sensed by the Kinect

6.1.2 *Create a Patient-Specific Vibrotactile Interface*

Using data collected from the robotic mapping technique, it would be possible to design custom vibrotactile arrays that fit over the TMR site with maximum resolution. The stimulation and sensation parameters collected can be used to develop a control algorithm that translates data from sensors on the prosthesis to actuation signals provided at the TMR site. To the best of our knowledge, no wearable interface has been developed to stimulate sensation at a TMR site nor have any studies been published to study this possibility.

Depending on the type of amputation and the post-operative anatomy of each subject, these arrays will have to fit inside a socket or sit above the socket. In both cases, mechanically integrating actuators into the gel liner would be the best design for ideal user interface. Other design considerations must also be taken into account such as size, weight, salience, and usability.

Once the device is made, validation of this sensory feedback system will test to see if patients can accurately identify the sensations that are being triggered by the prosthesis. This would be followed by a more comprehensive study to quantify how sensory feedback from prosthetic legs can benefit lower-limb amputees in their day-to-day lives.

BIBLIOGRAPHY

[1] J. . Nielsen and T. Sinkjaer, "Afferent feedback in the control of human gait," *J. Electromyogr. Kinesiol.*, vol. 12, no. 3, pp. 213–217, Jun. 2002.

[2] Y. Lajoie, N. Teasdale, J. D. Cole, M. Burnett, C. Bard, M. Fleury, R. Forget, J. Paillard, and Y. Lamarre, "Gait of a deafferented subject without large myelinated sensory fibers below the neck.," *Neurology*, vol. 47, no. 1, pp. 109–115, 1996.

[3] K. Ziegler-Graham, E. J. MacKenzie, P. L. Ephraim, T. G. Travison, and R. Brookmeyer, "Estimating the Prevalence of Limb Loss in the United States: 2005 to 2050," *Arch. Phys. Med. Rehabil.*, vol. 89, no. 3, pp. 422–429, 2008.

[4] M. F. Owings and L. J. Kozak, "Ambulatory and inpatient procedures in the United States, 1996," *Data from Natl. Heal. Surv.*, vol. 139, pp. 1–119, 1998.

[5] D. Rusaw, K. Hagberg, L. Nolan, and N. Ramstrand, "Can vibratory feedback be used to improve postural stability in persons with transtibial limb loss?," *J. Rehabil. Res. Dev.*, vol. 49, no. 8, p. 1239, 2012.

[6] E. C. Wentink, *Feasibility of enhanced user control and feedback in upper leg prostheses*. Enschede, The Netherlands, 2013.

[7] V. Ramachandran, M. Stewart, and D. Rogers-Ramachandran, "Perceptual correlates of massive cortical reorganization," *Neroreport*, vol. 3, no. 7, pp. 583–586, 1992.

[8] a Karl, N. Birbaumer, W. Lutzenberger, L. G. Cohen, and H. Flor, "Reorganization of motor and somatosensory cortex in upper extremity amputees with phantom limb pain.," *J. Neurosci.*, vol. 21, no. 10, pp. 3609–3618, 2001.

[9] E. L. Simoes, I. Bramati, E. Rodrigues, a. Franzoi, J. Moll, R. Lent, and F. Tovar-Moll, "Functional Expansion of Sensorimotor Representation and Structural Reorganization of Callosal Connections in Lower Limb Amputees," *J. Neurosci.*, vol. 32, no. 9, pp. 3211–3220, 2012.

[10] H. Herr and R. Kornbluh, "New horizons for orthotic and prosthetic technology: artificial muscle for ambulation," *Smart Struct. Mater. Electroact. Polym. Actuators Devices*, vol. 5385, pp. 1–9, 2004.

[11] R. Versluys, P. Beyl, M. Van Damme, A. Desomer, R. Van Ham, and D. Lefeber, "Prosthetic feet: state-of-the-art review and the importance of mimicking human ankle-foot biomechanics.," *Disabil. Rehabil. Assist. Technol.*, vol. 4, no. 2, pp. 65–75, 2009.

[12] W. C. Miller, M. Speechley, and B. Deathe, "The prevalence and risk factors of falling and fear of falling among lower extremity amputees.," *Arch. Phys. Med. Rehabil.*, vol. 82, no. 8, pp. 1031–7, Aug. 2001.

[13] W. C. Miller, a B. Deathe, M. Speechley, and J. Koval, "The influence of falling, fear of falling, and balance confidence on prosthetic mobility and social activity among individuals with a lower extremity amputation.," *Arch. Phys. Med. Rehabil.*, vol. 82, no. 9, pp. 1238–44, Sep. 2001.

[14] W. Miller and A. Deathe, "A prospective study examining balance confidence among individuals with lower limb amputation," *Disabil. Rehabil.*, vol. 26, no. 14–15, pp. 875–881, Jan. 2004.

[15] W. C. Miller, M. Speechley, and A. B. Deathe, "Research Report With Lower-Limb Amputations," pp. 856–865, 2014.

[16] S. Knecht, H. Henningsen, C. Höhling, T. Elbert, H. Flor, C. Pantev, and E. Taub, "Plasticity of plasticity? Changes in the pattern of perceptual correlates of reorganization after amputation," *Brain*, vol. 121, no. 4, pp. 717–724, 1998.

[17] V. Ramachandran and W. Hirstein, "The perception of phantom limb," *Brain*, vol. 121, pp. 1603–30, 1998.

[18] M. J. Giummarra, S. J. Gibson, N. Georgiou-Karistianis, and J. L. Bradshaw, "Central mechanisms in phantom limb perception: The past, present and future," *Brain Res. Rev.*, vol. 54, no. 1, pp. 219–232, 2007.

[19] P. Montoya, W. Larbig, N. Grulke, H. Flor, E. Taub, and N. Birbaumer, "The relationship of phantom limb pain to other phantom limb phenomena in upper extremity amputees," *Pain*, vol. 72, no. 1–2, pp. 87–93, 1997.

[20] S. M. Grüsser, W. Mühlnickel, M. Schaefer, K. Villringer, C. Christmann, C. Koeppe, and H. Flor, "Remote activation of referred phantom sensation and cortical reorganization in human upper extremity amputees," *Exp. Brain Res.*, vol. 154, no. 1, pp. 97–102, 2004.

[21] P. D. Marasco, A. E. Schultz, and T. a. Kuiken, "Sensory capacity of reinnervated skin after redirection of amputated upper limb nerves to the chest," *Brain*, vol. 132, no. 6, pp. 1441–1448, 2009.

[22] T. a Kuiken, P. D. Marasco, B. a Lock, R. N. Harden, and J. P. a Dewald, "Redirection of cutaneous sensation from the hand to the chest skin of human amputees with targeted reinnervation.," *Proc. Natl. Acad. Sci. U. S. A.*, vol. 104, no. 50, pp. 20061–20066, 2007.

[23] P. D. Marasco, K. Kim, J. E. Colgate, M. a. Peshkin, and T. a. Kuiken, "Robotic touch shifts perception of embodiment to a prosthesis in targeted reinnervation amputees," *Brain*, vol. 134, no. 3, pp. 747–758, 2011.

[24] D. W. Tan, M. A. Schiefer, M. W. Keith, J. R. Anderson, J. Tyler, and D. J. Tyler, "NEUROPROSTHETICS A neural interface provides long-term stable natural touch perception," vol. 6, no. 257, 2014.

[25] C. Wall and E. Kentala, "Control of sway using vibrotactile feedback of body tilt in patients with moderate and severe postural control deficits," vol. 15, pp. 313–325, 2005.

[26] A. D. Goodworth, C. Wall, and R. J. Peterka, "Influence of Feedback Parameters on Performance of a Vibrotactile Balance Prosthesis," *IEEE Trans. Neural Syst. Rehabil. Eng.*, vol. 17, no. 4, pp. 397–408, 2009.

[27] K. H. Sienko, M. D. Balkwill, L. I. E. Oddsson, and C. Wall, "Effects of multi-directional vibrotactile feedback on vestibular-deficient postural performance during continuous multi-directional support surface perturbations," vol. 18, pp. 273–285, 2008.

[28] R. J. Peterka, C. Wall, E. Kentala, M. Eye, and E. Infirmary, "Determining the effectiveness of a vibrotactile balance prosthesis," vol. 16, pp. 45–56, 2006.

[29] P. P. Kadkade, B. J. Benda, P. B. Schmidt, and C. Wall, "Vibrotactile display coding for a balance prosthesis.," *IEEE Trans. Neural Syst. Rehabil. Eng.*, vol. 11, no. 4, pp. 392–9, Dec. 2003.

[30] C. Wall and M. S. Weinberg, "Balance Prostheses for Postural Control," *IEEE Eng. Med. Biol.*, no. April, 2003.

[31] F. Asseman, A. M. Bronstein, and M. a Gresty, "Using vibrotactile feedback of instability to trigger a forward compensatory stepping response.," *J. Neurol.*, vol. 254, no. 11, pp. 1555–61, Nov. 2007.

[32] F. Asseman, A. M. Bronstein, and M. A. Gresty, "Effectiveness of a Vibro-tactile Feedback to Cue a Stepping Response to a Balance Challenge .," in *IEEE International Workshop on Haptic Audio Visual Environments and their Applications*, 2006, no. November, pp. 4–6.

[33] E. C. Wentink, E. J. Talsma-Kerkdijk, H. S. Rietman, and P. Veltink, "Feasibility of error-based electrotactile and auditive feedback in prosthetic walking.," *Prosthet. Orthot. Int.*, Feb. 2014.

[34] W. K. Vos, D. G. Buma, and P. H. Veltink, "Optimisation of Spatial Electrocutaneous Display Parameters for Sensory Substitution," *EuroHaptics 2004*, pp. 123–128, 2004.

[35] R. E. Fan, S. Member, C. Wottawa, A. Mulgaonkar, R. J. Boryk, T. C. Sander, M. P. Wyatt, E. Dutson, W. S. Grundfest, and M. O. Culjat, "Pilot Testing of a Haptic Feedback Rehabilitation System on a Lower-limb Amputee," 2009.

[36] R. E. Fan, M. O. Culjat, C.-H. King, M. L. Franco, R. Boryk, J. W. Bisley, E. Dutson, and W. S. Grundfest, "A haptic feedback system for lower-limb prostheses.," *IEEE Trans. Neural Syst. Rehabil. Eng.*, vol. 16, no. 3, pp. 270–7, Jun. 2008.

[37] S. Crea, C. Cipriani, M. Donati, M. Carrozza, and N. Vitiello, "Providing time-discrete gait information by wearable feedback apparatus for lower-limb amputees: usability and functional validation.," *IEEE Trans. Neural Syst. Rehabil. Eng.*, vol. 4320, no. c, pp. 1–9, Oct. 2014.

[38] E. C. Wentink, a Mulder, J. S. Rietman, and P. H. Veltink, "Vibrotactile stimulation of the upper leg: effects of location, stimulation method and habituation.," *Conf. Proc. ... Annu. Int. Conf. IEEE Eng. Med. Biol. Soc. IEEE Eng. Med. Biol. Soc. Annu. Conf.*, vol. 2011, pp. 1668–71, Jan. 2011.

[39] A. Sharma, R. Torres-Moreno, K. Zabjek, and J. Andrysek, "Toward an artificial sensory feedback system for prosthetic mobility rehabilitation: examination of sensorimotor responses.," *J. Rehabil. Res. Dev.*, vol. 51, no. 6, pp. 907–17, Jan. 2014.

[40] C. Chapman, M. Bushnell, D. Miron, G. Duncan, and J. Lund, "Sensory perception during movement in man," *Exp. brain Res.*, vol. 68, no. 3, pp. 516–524, 987.

[41] D. K. Won, "How Sensation Occurs."

[42] M. Grunwald, *Human Haptic Perception: Basics and applications*. Springer Science & Business Media, 2008.

[43] T. Järvilehto, H. Hämäläinen, and K. Soininen, "Peripheral neural basis of tactile sensations in man: II. Characteristics of human mechanoreceptors in the hairy skin and correlations of their activity with tactile sensations.," *Brain Res.*, vol. 219, no. 1, pp. 13–27, 1981.

[44] R. S. Johansson and a. B. Vallbo, "Spatial properties of the population of mechanoreceptive units in the glabrous skin of the human hand," *Brain Res.*, vol. 184, no. 2, pp. 353–366, 1980.

[45] T. Liukkonen, "Human Reaction Times as a Response to Delays in Control Systems-Notes in vehicular context," *Kajaani Unit Dep. Inf. Process. Sci. Univ. Oulu*, 2009.

[46] M. Knibestol and A. B. Vallbo, "Single unit analysis of mechanoreceptor activity from the human glabrous skin," *Acta Physiol. Scand.*, vol. 80, no. 2, pp. 178–195, 1970.

[47] A. Van Lommel, *From cells to organs: a histology textbook and atlas*. Springer Science & Business Media, 2003.

[48] D. Purves, *Principles of cognitive neuroscience*. Sinauer Associates Inc., 2008.

[49] a W. Goodwin, B. D. Youl, and N. P. Zimmerman, "Single quickly adapting mechanoreceptive afferents innervating monkey glabrous skin: response to two vibrating probes.," *J. Neurophysiol.*, vol. 45, no. 2, pp. 227–242, 1981.

[50] R. S. Johansson, "Responses of mechanoreceptive afferent units in the glabrous skin of the human hand to sinusoidal skin displacements," *Brain Res.*, vol. 244, no. 1, pp. 17–25, 1982.

[51] E. R. Kandel, J. H. Schwartz, and T. M. Jessell, *Principles of neural science*, Vol 4. New York: McGraw-Hill, 2000.

[52] "ViviTouch." [Online]. Available: vivitouch.com.

[53] J. Bell-Krotoski, S. Weinstein, and C. Weinstein, "Testing sensibility, including touch-pressure, two-point discrimination, point localization, and vibration.," *J. Hand Ther.*, vol. 6, no. 2, pp. 114–123.

[54] S. Coren, *Sensation and Perception*. John Wiley & Sons, Inc., 2003.

[55] P. Agache, C. Monneur, J. Leveque, and J. De Rigal, "Mechanical Properties and Young's Modulus of Human Skin in Vivo," *Arch. Dermatol. Res.*, vol. 269, pp. 221–232, 1980.

[56] A. Hajian and R. Howe, "Identification of the mechanical impedance at the human finger tip," *J. Biomech. Eng.*, vol. 119, 1997.

[57] R. T. Verrillo, "Vibrotactile thresholds for hairy skin," *J. Exp. Psychol.*, vol. 72, no. 1, pp. 47–50, 1966.

[58] R. Lundstrom, "Local vibrations-mechanical impedance human hand's glabrous skin," *J. Biomech.*, vol. 17, no. 2, pp. 137–144, 1984.

[59] T. Moore and J. Mundie, "Measurement of Specific Mechanical Impedance of the Skin : TRANSD / CER," *J. Acoust. Soc. Am.*, vol. 4, no. 16, 1972.

[60] M. Fritschi, K. Drewing, R. Zopf, M. O. Ernst, and M. Buss, "Construction and first evaluation of a newly developed tactile shear force display," *Proc. 4th ...*, pp. 508–511, 2004.

[61] F. M. Hendriks, D. Brokken, J. T. W. M. van Eemeren, C. W. J. Oomens, F. P. T. Baaijens, and J. B. a M. Horsten, "A numerical-experimental method to characterize the non-linear mechanical behaviour of human skin.," *Ski. Res. Technol.*, vol. 9, no. 3, pp. 274–83, 2003.

[62] J. Lindsay, R. J. Adams, and B. Hannaford, "Improving Tactile Feedback with an Impedance Adapter," pp. 713–718.

[63] E. K. Franke, “Mechanical impedance of the surface of the human body,” *J. Appl. Physiol.*, vol. 3, no. 10, pp. 582–590, 1951.

[64] “Scilab,” *2012*. [Online]. Available: http://www.scilab.org.

[65] B. J. Kemp, “Reaction time of young and elderly subjects in relation to perceptual deprivation and signal-on versus signal-off sonditions,” *Dev. Psychol.*, vol. 8, no. 2, p. 268, 1973.

[66] W. H. Marshall, S. A. Talbot, and H. W. Ades, “Cortical response of the anesthetized cat to gross photic and electrical afferent stimulation,” *J. Neurophysiol.*, vol. 6, no. 1, pp. 1–15, 1943.

[67] E. S. Robinson, “Work of the Integrated Organism,” 1934.

[68] S. AF and S. A, *Elements of human performance: Reaction processes and attention in human skill*. 2013.

[69] F. C. Donders, “On the speed of mental processes.,” *Acta Psychol. (Amst).*, vol. 30, pp. 412–431, 1969.

[70] D. R. J. Laming, “Information theory of choice-reaction times,” 1968.

[71] A. Welford, “Reaction Times,” *Acad. Press*, 1980.

[72] W. H. Teichner, “Laws of visual choice reaction time,” *Psychol. Rev.*, vol. 81, no. 1, p. 75, 1974.

[73] R. D. Luce, *Response times*, No. 8. Oxford University Press, 1986.

[74] W. W. Surwillo, “Choice reaction time and speed of information processing in old age,” *Percept. Mot. Skills*, vol. 36, no. 1, pp. 231–322, 1973.

[75] W. E. Hick, “On the rate of gain of information,” *Q. J. Exp. Psychol.*, vol. 4, no. 1, pp. 11–26, 1952.

[76] S. Sternberg, “Memory-scanning: Mental processes revealed by reaction-time experiments,” *Am. Sci.*, pp. 421–457, 1969.

[77] R. S. Nickerson, “Binary-classification reaction time: A review of some studies of human information-processing capabilities,” *Psychon. Monogr. Suppl.*, 1972.

[78] W. Berger, J. Quintern, and V. Dietz, “Stance and gait perturbations in children: developmental aspects of compensatory mechanisms.,” *Electroencephalogr. Clin. Neurophysiol.*, vol. 61, no. 5, pp. 385–395, 1985.

[79] D. A. Winter, “Human balance and posture control during standing and walking,” *Gait Posture*, vol. 3, no. 4, pp. 193–214, 1995.

[80] M. Pijnappels, M. F. Bobbert, and J. H. van Dieën, “EMG modulation in anticipation of a possible trip during walking in young and older adults.,” *J. Electromyogr. Kinesiol.*, vol. 16, no. 2, pp. 137–43, Apr. 2006.

[81] M. Pijnappels, M. F. Bobbert, and J. H. Van Dieën, “How early reactions in the support limb contribute to balance recovery after tripping,” *J. Biomech.*, vol. 38, no. 3, pp. 627–634, 2005.

[82] C. Curtze, A. L. Hof, B. Otten, and K. Postema, “Balance recovery after an evoked forward fall in unilateral transtibial amputees,” *Gait Posture*, vol. 32, no. 3, pp. 336–341, 2010.

[83] C. E. Stepp, Q. An, and Y. Matsuoka, “Repeated training with augmentative vibrotactile feedback increases object manipulation performance,” *PLoS One*, vol. 7, no. 2, 2012.

[84] L. R. Elliott, A. Skinner, R. A. Pettitt, and J. Vice, “Utilizing Glove-Based Gestures and a Tactile Vest Display for Covert Communications and Robot Control,” no. June, 2014.

[85] J. J. Scott and R. Gray, “A comparison of tactile, visual, and auditory warnings for rear-end collision prevention in simulated driving.,” *Hum. Factors*, vol. 50, no. 2, pp. 264–275, 2008.

[86] J. B. F. Van Erp and H. a H. C. Van Veen, “Vibrotactile in-vehicle navigation system,” *Transp. Res. Part F Traffic Psychol. Behav.*, vol. 7, no. 4–5, pp. 247–256, 2004.

[87] S. Luck, G. F. Woodman, and E. K. Vogel, “Event-related potential studies of attention,” *Trends Cogn. Sci.*, vol. 4, no. 11, pp. 432–440, 2000.

[88] D. R. E., “In-vehicle information and driver overload,” *Int. J. Veh. Des.*, vol. 9, no. 1981, pp. 557–564, 1988.

[89] R. J. Kosinski, “Literature Review on Reaction Time,” 2013. [Online]. Available: http://biae.clemson.edu/bpc/bp/lab/110/reaction.htm. [Accessed: 25-Mar-2015].

[90] J. L. Fozard, M. Vercruyssen, S. L. Reynolds, P. A. Hancock, and R. E. Quilter, “Age Differences and Changes in Reaction Time: The Baltimore Longitudinal Study of Aging,” *J. Gerontol.*, vol. 49, no. 4, pp. P179–P189, Jul. 1994.

[91] F. Khoshnoud and C. W. De Silva, “Recent advances in MEMS sensor technology-mechanical applications,” *IEEE Instrum. Meas. Mag.*, vol. 15, no. 2, pp. 14–24, 2012.

[92] A. Sieber, P. Valdastri, K. Houston, C. Eder, O. Tonet, A. Menciassi, and P. Dario, "A novel haptic platform for real time bilateral biomanipulation with a MEMS sensor for triaxial force feedback," *Sensors Actuators, A Phys.*, vol. 142, no. 1, pp. 19–27, 2008.

[93] P. Fortin, M. J.-D. Otis, V. Duchaine, and J. R. Cooperstock, "Event-based haptic vibration synthesis using a recursive filter for lower limb prosthetics," *2014 IEEE Int. Symp. Haptic, Audio Vis. Environ. Games Proc.*, pp. 47–52, Oct. 2014.

[94] A. Barghout, J. Cha, A. E. Saddik, J. Kammerl, and E. Steinbach, "Spatial resolution of vibrotactile perception on the human forearm when exploiting funneling illusion," *2009 IEEE Int. Work. Haptic Audio Vis. Environ. Games, HAVE 2009 - Proc.*, pp. 19–23, 2009.

[95] C. Wall, M. S. Weinberg, P. B. Schmidt, and D. E. Krebs, "Balance prosthesis based on micromechanical sensors using vibrotactile feedback of tilt.," *IEEE Trans. Biomed. Eng.*, vol. 48, no. 10, pp. 1153–61, Oct. 2001.

[96] F. Mancini, A. Bauleo, J. Cole, F. Lui, C. a. Porro, P. Haggard, and G. D. Iannetti, "Whole-body mapping of spatial acuity for pain and touch," *Ann. Neurol.*, vol. 75, no. 6, pp. 917–924, 2014.

[97] S. Millar, "Memory in touch," *Psicothema*, vol. 11, no. 4, pp. 747–767, 1999.

[98] A. L. Kaas, H. Van Mier, and R. Goebel, "The neural correlates of human working memory for haptically explored object orientations," *Cereb. Cortex*, vol. 17, no. 7, pp. 1637–1649, 2007.

[99] R.-S. Huang, C. -f. Chen, a. T. Tran, K. L. Holstein, and M. I. Sereno, "Mapping multisensory parietal face and body areas in humans," *Proc. Natl. Acad. Sci.*, vol. 109, no. 44, pp. 18114–18119, 2012.

[100] S. J. Graham, W. R. Staines, a. Nelson, D. B. Plewes, and W. E. McIlroy, "New devices to deliver somatosensory stimuli during functional MRI," *Magn. Reson. Med.*, vol. 46, no. 3, pp. 436–442, 2001.

[101] G. S. Harrington, C. T. Wright, and J. H. Downs, "A new vibrotactile stimulator for functional MRI," *Hum. Brain Mapp.*, vol. 10, no. 3, pp. 140–145, 2000.

[102] G. S. Harrington and J. Hunter Downs Iii, "FMRI mapping of the somatosensory cortex with vibratory stimuli: Is there a dependency on stimulus frequency?," *Brain Res.*, vol. 897, no. 1–2, pp. 188–192, 2001.

[103] S. T. Francis, E. F. Kelly, R. Bowtell, W. J. Dunseath, S. E. Folger, and F. McGlone, "fMRI of the responses to vibratory stimulation of digit tips.," *Neuroimage*, vol. 11, no. 3, pp. 188–202, 2000.

[104] E. R. Gizewski, O. Koeze, K. Uffmann, A. De Greiff, M. E. Ladd, and M. Forsting, "Cerebral activation using a MR-compatible piezoelectric actuator with adjustable vibration frequencies and in vivo wave propagation control," *Neuroimage*, vol. 24, no. 3, pp. 723–730, 2005.

[105] F. Mcglone, E. F. Kelly, M. Trulsson, S. T. Francis, and R. Bowtell, "Functional neuroimaging studies of human somatosensory cortex," *Most*, vol. 135, 2002.

[106] R. S. Huang and M. I. Sereno, "Dodecapus: An MR-compatible system for somatosensory stimulation," *Neuroimage*, vol. 34, no. 3, pp. 1060–1073, 2007.

[107] R. W. Briggs, I. Dy-Liacco, M. P. Malcolm, H. Lee, K. K. Peck, K. S. Gopinath, N. C. Himes, D. a. Soltysik, P. Browne, and R. Tran-Son-Tay, "A Pneumatic Vibrotactile Stimulation Device for fMRI," *Magn. Reson. Med.*, vol. 51, no. 3, pp. 640–643, 2004.

[108] S. M. Golaszewski, F. Zschiegner, C. M. Siedentopf, J. Unterrainer, R. a. Sweeney, W. Eisner, S. Lechner-Steinleitner, F. M. Mottaghy, and S. Felber, "A new pneumatic vibrator for functional magnetic resonance imaging of the human sensorimotor cortex," *Neurosci. Lett.*, vol. 324, no. 2, pp. 125–128, 2002.

[109] S. a. Overduin and P. Servos, "Distributed digit somatotopy in primary somatosensory cortex," *Neuroimage*, vol. 23, no. 2, pp. 462–472, 2004.

[110] C. Stippich, R. Hofmann, D. Kapfer, E. Hempel, S. Heiland, O. Jansen, and K. Sartor, "Somatotopic mapping of the human primary somatosensory cortex by fully automated tactile stimulation using functional magnetic resonance imaging," *Neurosci. Lett.*, vol. 277, no. 1, pp. 25–28, 1999.

[111] M. F. Nolan, "Limits of two-point discrimination ability in the lower limb in young adult men and women.," *Phys. Ther.*, vol. 63, pp. 1424–1428, 1983.

[112] S. Millar and Z. Al-Attar, "External and body-centered frames of reference in spatial memory: evidence from touch.," *Percept. Psychophys.*, vol. 66, no. 1, pp. 51–59, 2004.

[113] "Dermatome (anatomy)," *Wikipedia*. [Online]. Available: http://en.wikipedia.org/wiki/Dermatome_%28anatomy%29.

[114] M. R. Feneley, J. W. Fawcett, and R. J. Keynes, "The role of Schwann cells in the regeneration of peripheral nerve axons through muscle basal lamina grafts," *Exp. Neurol.*, vol. 114, no. 3, pp. 275–285, 1991.

[115] D. J. Wigston and S. P. Donahue, "The location of cues promoting selective reinnervation of axolotl muscles.," *J. Neurosci.*, vol. 8, no. 9, pp. 3451–3458, 1988.

[116] D. J. Wigston and P. R. Kennedy, "Selective reinnervation of transplanted muscles by their original motoneurons in the axolotl.," *J. Neurosci.*, vol. 7, no. 6, pp. 1857–1865, 1987.

[117] D. J. Wigston and J. R. Sanes, "Selective reinnervation of intercostal muscles transplanted from different segmental levels to a common site.," *J. Neurosci.*, vol. 5, no. 5, pp. 1208–1221, 1985.

[118] T. a Kuiken, G. a Dumanian, R. D. Lipshutz, L. a Miller, and K. a Stubblefield, "The use of targeted muscle reinnervation for improved myoelectric prosthesis control in a bilateral shoulder disarticulation amputee," *Prosthet. Orthot. Int.*, vol. 28, pp. 245–253, 2004.

[119] K. D. O'Shaughnessy, G. a Dumanian, R. D. Lipschutz, L. a Miller, K. Stubblefield, and T. a Kuiken, "Targeted reinnervation to improve prosthesis control in transhumeral amputees. A report of three cases.," *J. Bone Joint Surg. Am.*, vol. 90, no. 2, pp. 393–400, 2008.

[120] T. a Kuiken, G. Li, B. a Lock, R. D. Lipschutz, L. a Miller, K. a Stubblefield, and K. B. Englehart, "Targeted muscle reinnervation for real-time myoelectric control of multifunction artificial arms.," *JAMA*, vol. 301, no. 6, pp. 619–628, 2009.

[121] L. J. Hargrove, A. M. Simon, A. J. Young, R. D. Lipschutz, S. B. Finucane, D. G. Smith, and T. a Kuiken, "Robotic leg control with EMG decoding in an amputee with nerve transfers.," *N. Engl. J. Med.*, vol. 369, no. 13, pp. 1237–42, 2013.

[122] S. Agnew, A. Shultz, G. Dumanian, and T. Kuiken, "Targeted reinnervation in the transfemoral amputee: A preliminary study of surgical technique," *Plast. Reconstr. Surg.*, vol. 129, no. 1, pp. 187–194, 2012.

[123] L. J. Hargrove, A. M. Simon, R. D. Lipschutz, S. B. Finucane, and T. a. Kuiken, "Real-Time myoelectric control of knee and ankle motions for transfemoral amputees," *J. Am. Med. Assoc.*, vol. 305, no. 15, pp. 1542–1544, 2011.

[124] L. Nikolajsen, "Phantom limb pain," *Br. J. Anaesth.*, vol. 87, no. 1, pp. 107–116, 2001.

[125] H. Flor, L. Nikolajsen, and T. Staehelin Jensen, "Phantom limb pain: a case of maladaptive CNS plasticity?," *Nat. Rev. Neurosci.*, vol. 7, no. 11, pp. 873–881, 2006.

[126] a Hill, "Phantom limb pain: a review of the literature on attributes and potential mechanisms.," *J. Pain Symptom Manage.*, vol. 17, no. 2, pp. 125–142, 1999.

[127] P. Montoya, K. Ritter, E. Huse, W. Larbig, C. Braun, S. Töpfner, W. Lutzenberger, W. Grodd, H. Flor, and N. Birbaumer, "The cortical somatotopic map and phantom phenomena in subjects with congenital limb atrophy and traumatic amputees with phantom limb pain," *Eur. J. Neurosci.*, vol. 10, no. 3, pp. 1095–1102, 1998.

[128] L. a. Miller, R. D. Lipschutz, K. a. Stubblefield, B. a. Lock, H. Huang, T. W. Williams, R. F. Weir, and T. a. Kuiken, "Control of a Six Degree of Freedom Prosthetic Arm After Targeted Muscle Reinnervation Surgery," *Arch. Phys. Med. Rehabil.*, vol. 89, no. 11, pp. 2057–2065, 2008.

[129] T. a. Kuiken, L. a. Miller, R. D. Lipschutz, B. a. Lock, K. Stubblefield, P. D. Marasco, P. Zhou, and G. a. Dumanian, "Targeted reinnervation for enhanced prosthetic arm function in a woman with a proximal amputation: a case study," *Lancet*, vol. 369, no. 9559, pp. 371–380, 2007.

[130] L. A. Miller, S. Member, K. A. Stubblefield, R. D. Lipschutz, B. A. Lock, T. A. Kuiken, and S. Member, "Improved myoelectric control using targeted reinnervation surgery a case series," vol. 16, no. 1, pp. 46–50, 2008.

[131] A. E. Schultz, P. D. Marasco, and T. a. Kuiken, "Vibrotactile detection thresholds for chest skin of amputees following targeted reinnervation surgery," *Brain Res.*, vol. 1251, pp. 121–129, 2009.

[132] H. Huang, P. Zhou, G. Li, and T. a. Kuiken, "An analysis of EMG electrode configuration for targeted muscle reinnervation based neural machine interface," *IEEE Trans. Neural Syst. Rehabil. Eng.*, vol. 16, no. 1, pp. 37–45, 2008.

[133] J. Souza, N. Fey, J. Cheesborough, S. Agnew, L. Hargrove, and G. Dumanian, "Advances in Transfemoral Amputee Rehabilitation: Early Experience with Targeted Muscle Reinnervation," *Curr. Surg. Reports*, vol. 2, no. 5, pp. 1–9, 2014.

[134] I. Jiang, Y. Ishikawa, J. Lindsay, and B. Hannaford, "Design and optimization of support structures for tactile feedback," in *2013 World Haptics Conference (WHC)*, 2013, pp. 485–490.

[135] D. Desmond and M. MacLachlan, "Psychosocial Issues in the Field of Prosthetics and Orthotics," *JPO J. Prosthetics Orthot.*, vol. 14, no. 1, pp. 19–22, 2002.

[136] B. Van Dorsten, "Integrating psychological and medical care: practice recommendations for amputation," *New York: Demos Medical Publishing, Inc.*, pp. 73–88, 2004.

[137] C. Murray, "Embodiment and prosthetics," *Psychoprosthetics*, pp. 119–129, 2008.

[138] B. Rybarczyk and J. Behel, "Limb loss and body image," *Psychoprosthetics*, pp. 23–31, 2008.

[139] B. Hannaford, J. Rosen, D. W. Friedman, H. King, P. Roan, L. Cheng, D. Glozman, J. Ma, S. N. Kosari, and L. White, "Raven-II: An open platform for surgical robotics research," *IEEE Trans. Biomed. Eng.*, vol. 60, no. 4, pp. 954–959, 2013.

[140] C. Layne, “Unit 4.” [Online]. Available: http://grants.hhp.coe.uh.edu/clayne/6397/unit4a.htm.

[141] Antranik, “Functional areas of the cerebral cortex,” 2011. [Online]. Available: http://antranik.org/functional-areas-of-the-cerebral-cortex/.

VITA

Iris Shing-Yi Jiang was born in 1988 and raised in Agoura Hills, California. She completed her Bachelor of Science in Bioengineering at the University of California, Berkeley in 2009. At Berkeley, she joined the He Lab, which influenced her to pursue graduate school. Iris joined the BioRobotics Laboratory in 2010 where she was advised by Professor Blake Hannaford. In 2015 she earned a Doctor of Philosophy degree in Bioengineering from the University of Washington.